INFLUENCE OF SOIL TYPE ON CONE PENETRATION RESISTANCE - SHEAR WAVE VELOCITY CORRELATION

A Thesis Submitted to
the Graduate School of
İzmir Institute of Technology
in Partial Fulfillment of the Requirements for Degree of

MASTER OF SCIENCE

in Civil Engineering

by
Murat ÖRÜCÜ

June 2022
İZMİR

ACKNOWLEDGMENTS

ABSTRACT

INFLUENCE OF SOIL TYPE ON CONE PENETRATION RESISTANCE - SHEAR WAVE VELOCITY CORRELATION

Many researchers proposed correlations between cone penetration resistance (q_c) and shear wave velocity (V_s). The researchers used the datasets they obtained by performing laboratory or field tests while developing their correlations. The q_c measurements were made with CPT test and V_s measurements were made with in-situ tests (SCPT, DHT, CHT). The proposed correlations were very different from each other. The existing correlations between q_c and V_s are given in two ways: The soil type-dependent correlations and different correlations for different soil types. The soil type-dependent correlations were limited and also there is no change depending on fines content . Therefore, it would be useful to determine a correlation based on soil type with soils with different fines content.

In this study, CPT and SCPT tests were performed in the getechnical laboratory of IZTECH to investigate the influence of soil type on q_c-V_s correlation. Tests were performed on clean sand and sand - non-plastic silt mixtures having 5%, 15%, and 35% fines content at different relative densities inside the soil box. CPT profiles and V_s values were obtained to develop a relationship between V_s, and q_c based on soil type index (I_c). The I_c values were found using CPT-based approaches found in the literature. A new soil type-dependent correlation to predict the V_s of soils from q_c is presented in this study. The new equation was compared with existing correlations. The equation is useful to estimate V_s from CPT measurements for all soil types with different fines content.

ÖZET

ZEMİN TİPİNİN KONİ PENETRASYON DİRENCİ - KAYMA DALGASI HIZI KORELASYONUNA ETKİSİ

Birçok araştırmacı, koni penetrasyon direnci (q_c) ile kayma dalgası hızı (V_s) arasında korelasyonlar önermiştir. Araştırmacılar korelasyonlarını geliştirirken laboratuvar veya saha testleri yaparak elde ettikleri veri setlerini kullanmışlardır. q_c ölçümleri CPT testi ile, V_s ölçümleri ise yerinde testler (SCPT, DHT, CHT) ile yapılmıştır. Önerilen korelasyonlar birbirinden çok farklıdır. q_c ve V_s arasındaki mevcut korelasyonlar iki şekilde verilmiştir: Zemin tipine bağlı korelasyonlar ve farklı zemin tipleri için farklı korelasyonlar. Zemin tipine bağlı korelasyonlar sınırlıdır ve ayrıca ince tane muhtevasına bağlı değişim yoktur. Bu nedenle, farklı ince tane muhtevasına sahip zeminler ile toprak tipine dayalı bir korelasyon belirlemek faydalı olacaktır.

Bu çalışmada, zemin tipinin q_c – V_s korelasyonu üzerindeki etkisini araştırmak için İYTE'nin geoteknik laboratuvarında CPT ve SCPT testleri yapılmıştır.Testler zemin kutusu içerisinde, farklı rölatif sıkılıklarda, temiz kuma ve 5%, 15%, and 35% ince tane muhtevasına sahip temiz kum-plastik olmayan silt karışımlarına uygulanmıştır. Toprak tipi indeksine (I_c) dayalı olarak V_s ve q_c arasında bir ilişki geliştirmek için CPT profilleri ve V_s değerleri elde edilmiştir. I_c değerleri, literatürde bulunan CPT tabanlı yaklaşımlar kullanılarak bulunmuştur. Bu çalışmada, koni penetrasyon direncinden zeminlerin kayma dalgası hızını tahmin etmek için zemin tipine bağlı yeni bir korelasyon sunulmaktadır. Yeni denklem mevcut korelasyonlarla karşılaştırılmıştır. Denklem, farklı ince tane muhtevasına sahip tüm zemin türleri için CPT ölçümlerinden kayma dalgası hızını tahmin etmek için faydalıdır.

TABLE OF CONTENTS

LIST OF FIGURES

LIST OF TABLES

CHAPTER 1

INTRODUCTION

1.1. Introduction and Scope of Study

The cone penetration test (CPT) is a standard in-situ test used to determine soil properties and structure. CPT provides fast, reliable, and continuous data, and it is economical are the features that make CPT attractive (Robertson, 2016). As a result of CPT tests, soil parameters such as tip resistance (q_c) and friction resistance (f_s) are obtained. Also, the pore water pressure can be obtained from the cone penetrating the ground using the piezocone penetration tests (CPTu). In geotechnical engineering, shear wave velocity (V_s) is an important parameter in defining the small-strain stiffness characteristics of soils (Tonni et al., 2013). Shear wave velocity is used to determine soil properties and the dynamic response of the soil. In the field, shear wave velocity is measured in situ tests such as seismic cone penetration test (SCPT), crosshole test (CHT), downhole test (DHT), suspension logger (SL), and spectral analysis of surface waves (SASW). Robertson et al. (1986) stated that standard shear wave tests such as CHT and DHT require one or more boreholes. Therefore, SCPT is generally preferred as it is a less costly application than other in situ tests. SCPT was developed from the cone penetration test (CPT), and actually it is the combination of the seismic downhole method and the CPT logging (Robertson et al., 1986). The test uses seismic equipment in addition to the CPT test. Generally, bender element (BE) tests are used in the laboratory for V_s measurements.

Identification and classification of soil type are primary applications of CPT results. The soil behavior type is obtained by interpreting the CPT results and is used for the classification of soils. Soil behavior type determination from CPT results has been the subject of many studies until today (Schmertmann, 1978; Robertson et al., 1986; Robertson, 1990). In general, soil behavior type has been tried to be determined by using CPT-based charts. Robertson and Wride (1998) defined the soil behavior type index (I_c) by developing an equation from the chart of Robertson (1990).

In this study, the effect of soil type on the relationship between cone penetration resistance (q_c) and shear wave velocity (V_s) was investigated by performing CPT and SCPT in the laboratory, and a soil type-dependent correlation between q_c and V_s was proposed. The CPT and SCPT tests were carried out on clean sand and non-plastic silt mixtures. Clean sand was obtained from the Urla district of İzmir. The non-plastic silt was taken from Babaeski region of Kırklareli. Sand and silt contained quaternary sediments (Ecemis et al., 2022). The experiments were applied to soils with four different silt ratios by weight at different relative densities in a soil box. These are clean sand, 5% silty sand, 15% silty sand, and 35% silty sand.

The relationship between q_c and V_s has been studied by many researchers to date (Baldi et al., 1989; Rix and Stokoe, 1991; Robertson et al., 1992; Hegazy and Mayne, 1995; Fear and Robertson, 1995; Mayne and Rix, 1995; Andrus et al., 2004; Hegazy and Mayne, 2006; Andrus et al., 2007; Robertson, 2009; Ecemis, 2020). Some of the researchers developed their correlations depending on the soil type (Hegazy and Mayne, 2006; Andrus et al., 2007; Robertson, 2009; Ecemis, 2020).

There are different correlations for different soils. Correlations were developed by performing laboratory and field experiments. Shear wave velocity was found by in-situ tests, and there was no SCPT test in the laboratory. A single type of soil was used in the experiments. Soils with different fines content (FC) were not used. A new soil type-dependent correlation to predict the V_s of soils from q_c is presented in this study. Shear wave measurements were made using SCPT tests in the laboratory. In the experiments, soils with FC values between 0 and 35 were used instead of single type of soils.

1.1. Thesis Organization

In this thesis, there are six chapters: Introduction, Literature Review, Preparation and Properties of Samples Used in the Experiments, Laboratory Study, Laboratory Test Results, and Conclusion.

Chapter 2 presents available studies/literature on determining the type of soil behavior from CPT results and available proposed correlations between q_c and V_s.

Chapter 3 describes the soil box, the preparation of the samples used in the experiments, and the sample properties.

Chapter 4 presents the laboratory study (CPT, SCPT), test equipment and test procedures.

Chapter 5 presents the laboratory test results. The chapter presents cone penetration resistance values obtained from CPT tests, shear wave velocity values obtained from SCPT tests, and soil type index values obtained by interpretation of CPT test results. The influence of soil type on the q_c - V_s correlation was investigated using all test results. Finally, a relationship between q_c and V_s based on soil type index has been proposed, and the proposed relationship is compared with other existing studies.

Chapter 6 presents the concluding part and suggestions.

CHAPTER 2

LITERATURE REVIEW

2.1. Introduction

The geological age, origin, composition, grain size, mineralogy, and soil history make the soil analysis complex and difficult, so data from cone penetration test and shear wave velocity tests should be correlated with each other to facilitate the analysis of soils (Karray et al., 2011). Parameters are obtained from cone penetration tests and shear wave velocity tests either directly during the test or by correcting or deriving the original data obtained (Lunne et al., 1997). Directly measured parameters are cone penetration resistance (q_c), friction resistance (f_s), pore water pressure, shear wave velocity (V_s), Corrected or derived parameters are friction ratio (F_r), normalized cone penetration resistance (q_{c1N}), soil behaviour type index (I_c) and normalized shear wave velocity (V_{s1}).

The relationship between q_c and V_s has been studied by many researchers to date (e.g., Baldi et al., 1989; Rix and Stokoe, 1991; Robertson et al., 1992; Hegazy and Mayne, 1995; Fear and Robertson, 1995; Mayne and Rix, 1995; Andrus et al., 2004; Hegazy and Mayne, 2006; Andrus et al., 2007; Robertson, 2009; Karray et al., 2011; Cai et al., 2014; Ecemis 2020). It was observed that cone penetration resistance, overburden stress, soil type, geological origin, and geological age affect the q_c-V_s correlation. Two types of correlation equations have been proposed by researchers, namely the soil type dependent correlation equations and the equations for different soil types. This chapter presents the place of soil type index in soil classification, interpretation of I_c by using CPT, and the correlations developed between CPT and V_s.

2.2. Soil behaviour type index

CPT has an important place in soil investigation because it is fast, repeatable, and economical, as well as provides continuous and precise data (Robertson, 2010). Identification and classification of soil type are major applications of CPT results. Soil classification is based on the interpretation of the soil behavior type (SBT) obtained from CPT results (Wair et al., 2012). Schmertmann (1978), Robertson et al. (1986), and Robertson (1990) stated that CPT-based charts are helpful in determining soil behavior type. Schmertmann (1978) and Robertson et al. (1986) proposed charts based on q_c, F_r and f_s. Robertson (1990) prepared his chart using overburden stress corrected parameters. The chart shown in Figure 2.1 is proposed by Robertson (1990) contained 9 SBTs and based on normalized cone penetration resistance (q_{c1N}) and normalized friction ratio (F_r). q_c and F_r are calculated by the equations given below;

$$q_{c1N} = \left(\frac{q_c}{P_a}\right)\left(\frac{P_a}{\sigma_{vo'}}\right)^n \tag{2.1}$$

$$F_r = \left[\frac{fs}{q_c - \sigma_{vo}}\right]100\% \tag{2.2}$$

Where P_a is the atmospheric pressure, σ_{vo}' is the effective stress, σ_{vo} is the total stress and n is the stress exponent. The stress exponent is defined by the equation given below (Robertson, 2009)

$$n = 0.381I_c + 0.05\left(\frac{\sigma_{vo'}}{P_a}\right) - 0.15 \tag{2.3}$$

Where I_c is soil behaviour type index. Robertson and Wride (1998) defined the I_c as radius of the boundaries between the SBTs in the chart. I_c is defined by the equation given below (Robertson and Wride, 1998)

$$I_c = [(3.47 - \log q_{c1})^2 + (\log F_r + 1.22)^2]^{0.5} \tag{2.4}$$

1. Sensitive, fine grained

2. Organic soils – peats

3. Clays – clay to silty clay

4. Silt mixtures – clayey silt to silty clay

5. Sand mixtures – silty sand to sandy silt

6. Sands – clean sand to silty sand

7. Gravelly sand to sand

8. Very stiff sand to clayey sand[*]

9. Very stiff, fine grained[*]

[*] Heavily overconsolidated or cemented
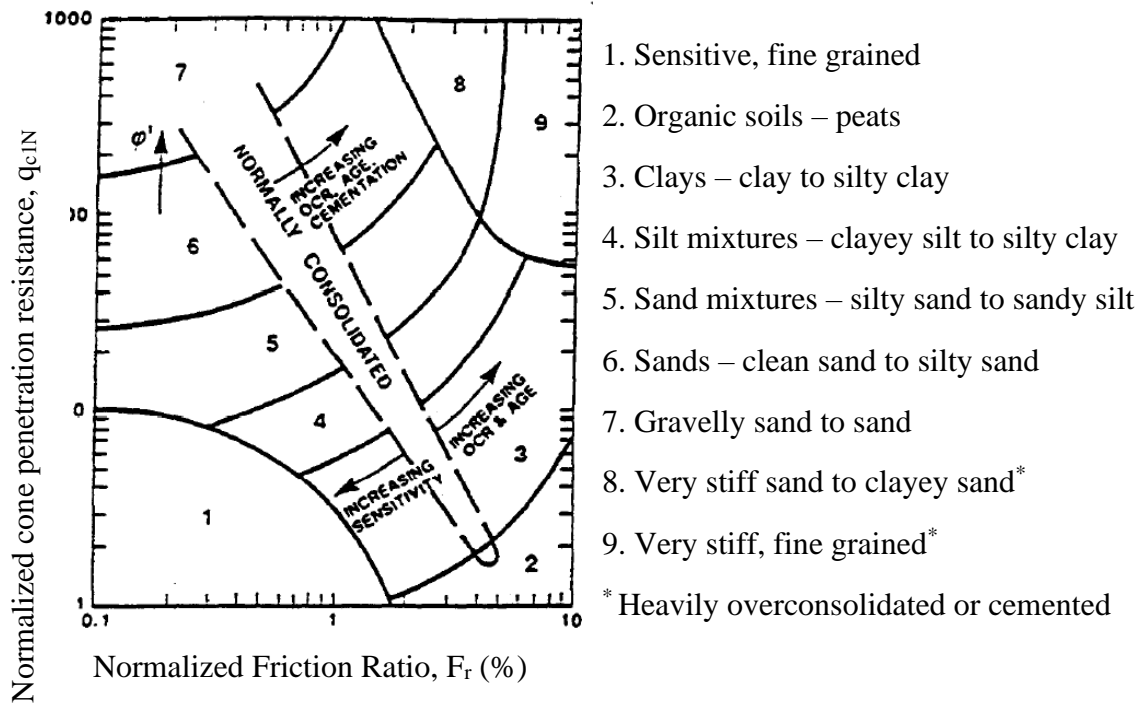
Figure 2.1. Soil behavior type classification chart

(Source: Robertson, 1990)

Table 2.1 shows the relationship between I_c and soil behaviour type developed by Robertson and Wride (1998).

Table 2.1. Relationship between I_c and soil behavior type developed by Robertson and Wride (1998).

Soil type index, I_c	Soil behavior type
$I_c < 1.31$	Gravelly sand to dense sand
$1.31 < I_c < 2.05$	Sands: clean sand to silty sand
$2.05 < I_c < 2.60$	Sand mixtures: silty sand to sandy silt
$2.60 < I_c < 2.95$	Silt mixtures: clayey silt to silty clay
$2.95 < I_c < 3.60$	Clays: silty clay to clay

6

2.3. Cone penetration resistance - shear wave velocity correlation

Many correlations between q_c and V_{s1} have been proposed up to date. Table 2.2 shows the existing correlations between CPT and V_{s1}. This table includes the soil type, V_s test type, and the number of data. The number of data indicates the number of data researchers have studied. The data word used in this part refers to the data set from the CPT and V_s measurements that the researchers used when developing the correlations.

Baldi et al. (1989) developed a relationship between V_s and q_c for uncemented silica sands with data obtained from Ticino sites in Italy. Resonant column test, and CPT calibration chamber test were performed to find the V_s and q_c values. Figure 2.2 shows the developed relationship between V_s and q_c for uncemented silica sands (Baldi et al., 1989). Assumptions are made to adjust the equations in the relationship given in the figure ($\sigma_{vo}' = 0.1$ MPa and $q_{c1N} = q_{c1} / Pa$)
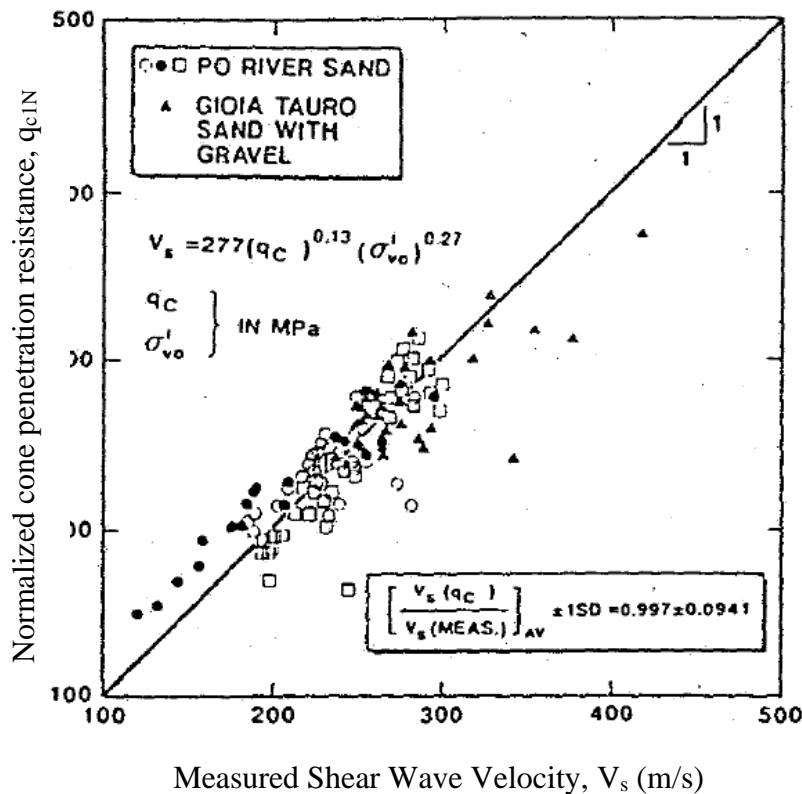
Figure 2.2. Relationships between V_s and q_c for uncemented silica sands

(Source: Baldi et al., 1989)

Rix and Stokoe (1991) proposed a correlation between G_{max} and q_c (Figure 2.3). Experimental data were obtained from washed mortar sand and Heber road sand deposits. The washed mortar sand is freshly deposited, poorly graded sand with FC of 1%. Heber road sand deposits contain three late Holocene age - uncemented sands with FC from 10% to 20%. Shear wave measurements were made using laboratory resonant column test for freshly deposited washed mortar sand and cross-hole test (CHT) for Heber road sand deposits. Assumptions are made to adjust the equations in the correlation given in the figure ($\sigma_{vo}' = 100$ kPa, $q_{c1N} = q_{c1} / Pa$ and $\gamma = 18.2$ kg -s^2/m^2).

$$\left[\frac{G_{max}}{q_c}\right]_{ave} \cong 1634 \left[\frac{q_c}{\sqrt{\sigma'_v}}\right]^{-0.75}$$

$$Range \cong Average \pm \frac{Average}{2}$$

$$\left.\begin{matrix} G_{max} \\ q_c \\ \sigma'_v \end{matrix}\right\} \text{ in kPa}$$
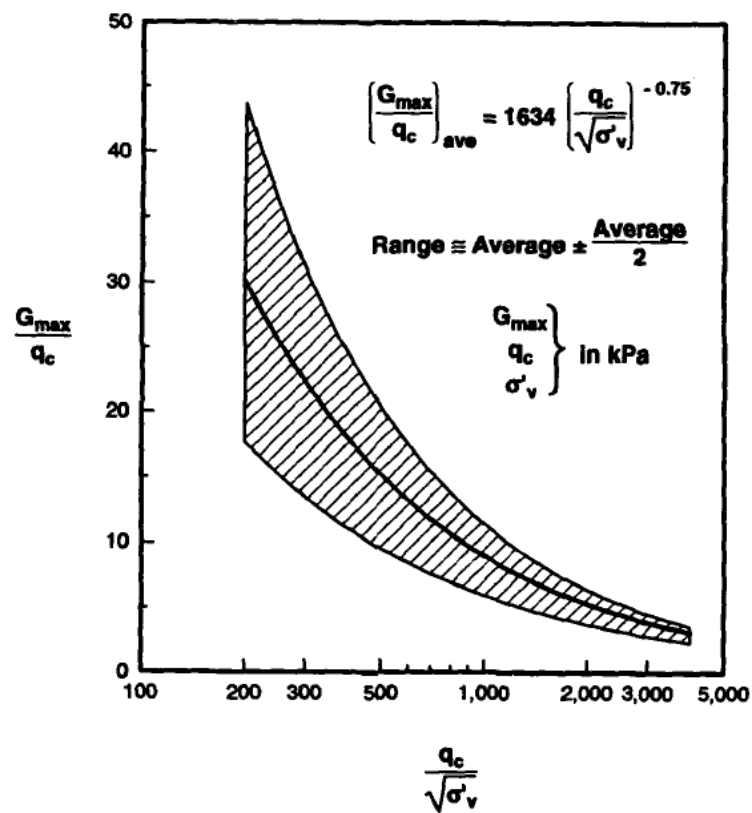
Figure 2. 3. Correlation between V_s and q_c for holocene sands
(Source: Rix and Stokoe, 1991)

Robertson et al. (1992) developed a relationship between CPT and V_{s1} with data from Fraser River Delta of British Columbia. They created a relationship given in Table 2.2 for young, uncemented silica clean sand using data obtained by performing in-situ tests. Shear wave measurements were made using a seismic cone penetration test (SCPT).

8

Hegazy and Mayne (1995) proposed a correlation between CPT and V_{s1} with data from 61 sites containing 24 sand sites, 36 clay sites, and one main tailing site. They suggested a correlation given in Table 2.2 for sand deposits with 133 test data, clay with 406 test data, and all soils with 323 test data obtained by performing in-situ tests. Shear wave measurements were made using seismic cone penetration test (SCPT), cross-hole test (CHT), downhole (DHT), and spectral analysis surface wave (SASW).

Fear and Robertson (1995) proposed the relationship between CPT and V_{s1} given in Table 2.2 for sand consisting of carbonate shell material containing 30% fines from the tailings sand site in Alaska. Shear wave velocity values were obtained from (SCPT).

Mayne and Rix (1995) developed a correlation between CPT and V_s for natural clays (8 <PI< 300), with 481 data taken from 31 different sites. Shear wave measurements were made using cross-hole test (CHT), downhole (DHT), and spectral analysis surface wave (SASW). Figure 2.4 shows the proposed relationship between V_s and q_c for clay by Mayne and Rix (1995).
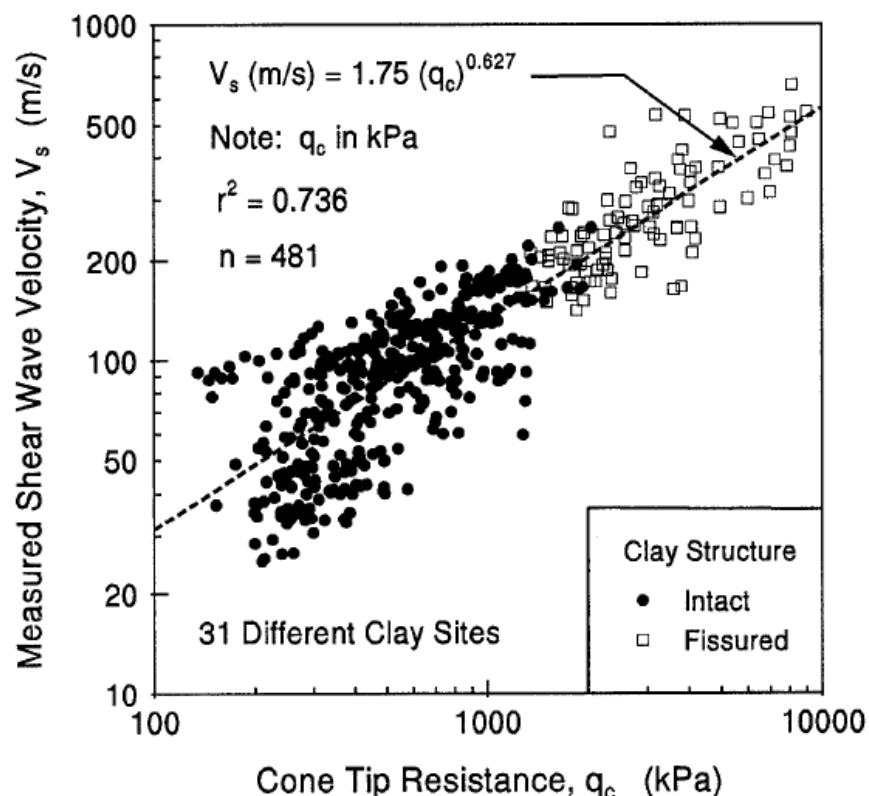
Figure 2. 4. Correlation between V_s and q_c for clays

(Source: Mayne and Rix, 1995)

Andrus et al. (2004) performed in-situ tests, studied 43 experimental data, and proposed a relationship between CPT and V_{s1} for Holocene age – unbounded soils. Twenty-two of the data are from California, seven from South Carolina, six from Canada, and eight from Japan. Shear wave measurements were made using seismic cone penetration test (SCPT) for 26 data, cross-hole test (CHT) for 6 data, suspension logger (SL) for 6 data, downhole (DHT) test for 2 data, and both SCPT and CHT for 3 data. Figure 2.5 shows the proposed relationship between V_{s1} and q_{c1N} for uncemented Holocene sands by Andrus et al. (2004).
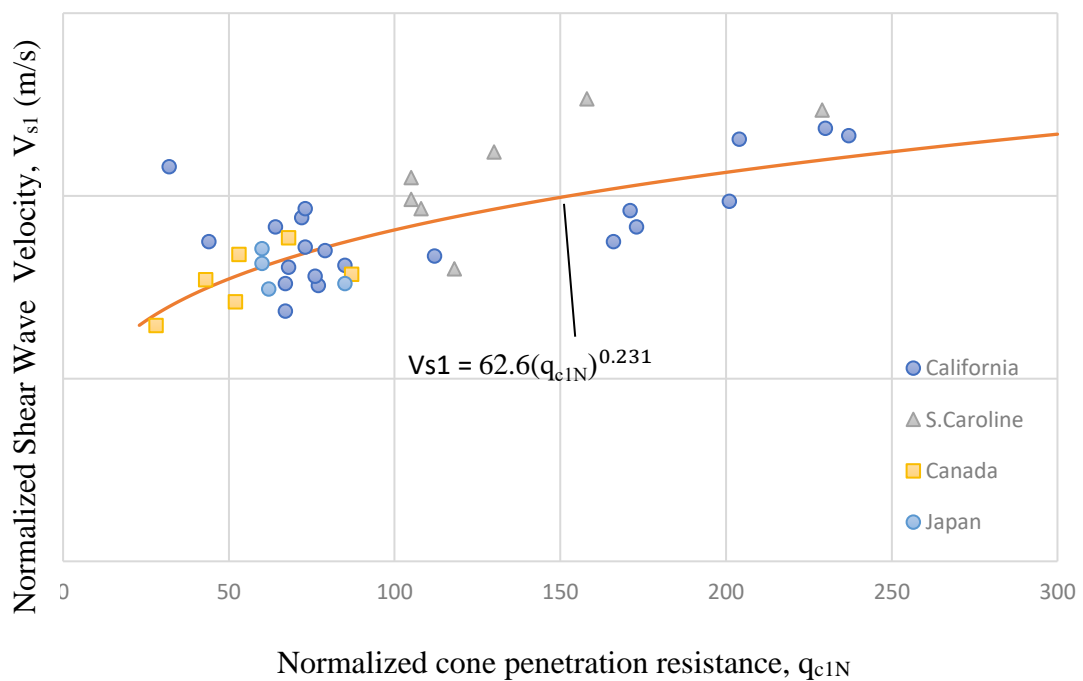
Figure 2. 5. Relationships between V_{s1} and q_{c1N} for uncemented holocene sands
(Source: Andrus et al., 2004)

Table 2.2. Existing correlations between CPT and V_{s1}

Study	V_{s1} (m/s)	Soil Type	Vs test type[a]	Number of Data Used
Baldi et al. (1989)	$110q_{c1N}^{0.13}$	Freshly deposited silica sands	Resonant column test	-
Rix and Stokoe (1991)	$123q_{c1N}^{0.125}$	Freshly deposited poorly graded sand and holocene age - uncemented sand deposits with FC from 10% to 20%.	Resonant column test, CHT	-
Robertson et al. (1992)	$60.3q_{c1N}^{0.23}$	Young,uncemented silica clean sand	SCPT	-
Hegazy and Mayne (1995)	$72.8q_{c1N}^{0.192}$	Sand deposites	SCPT, CHT, DHT, SASW	133
Fear and Robertson (1995)	$79.5q_{c1N}^{0.23}$	Sand consisting of carbonate shell material and containing 30% fines	SCPT	-
Mayne and Rix (1995)	$1.75q_{c1N}^{0.627}$, qc in kPa	Natural clays	CHT, DHT, SASW	481
Andrus et al. (2004)	$62.6q_{c1N}^{0.231}$	Uncemented holocene sand	SCPT, DHT, CHT, SL	43
Hegazy and Mayne (2006)	$0.0831q_{c1N}(e)^{1.786*I_c}$	All soil deposits	SCPT, CHT, DHT, SASW	558
Andrus et al. (2007)	$16.5(q_{c1N})^{0.411}I_c^{0.970}$	Holocene age sand		72
	$19.6(q_{c1N})^{0.396}I_c^{1.006}SF$ With SF = 1.11-1.12	Pleistocene age sand	SCPT, CHT, SL	113
	$115.2(q_{c1N})^{0.338}$	Tertiary age sand		44
Robertson (2009)	$(10^{0.55I_c+1.68}q_{c1N})^{0.5}$	Holocene and Pleistocene aged – uncemented silica soils	-	1035
Karray et al. (2011)	$149q_{c1}^{0.205}$	Péribonka site (uncemented and holocene age granular soils	MASW	900
Cai et al. (2014)	$38qc1^{0.61}$, q_{c1} in MPa	Clay deposits	SCPT, CHT, DHT, SASW	48
Ecemis (2020)	$\sqrt{(10)^{0.62I_c+1.35}q_{c1N}}$	Holocene–age unbounded soil	SCPT	115

[a] SCPT, seismic cone penetration test; DHT, downhole test; CHT, crosshole test; SL, suspension logger; SASW, spectral analysis surface wave.

Hegazy and Mayne (2006) developed a correlation between V_{s1} / q_{c1N} and I_c with data from 73 sites containing sand, clay, soil mixtures, and main tailing. The correlation was developed for all soils using a total of 558 data obtained by performing in-situ tests. Shear wave measurements were made using seismic cone penetration test (SCPT), cross-hole test (CHT), downhole (DHT), and spectral analysis surface wave (SASW). Figure 2.6 shows the results between V_{s1}/q_{c1N} and I_c, which expressed in the correlation by Hegazy and Mayne (2006).
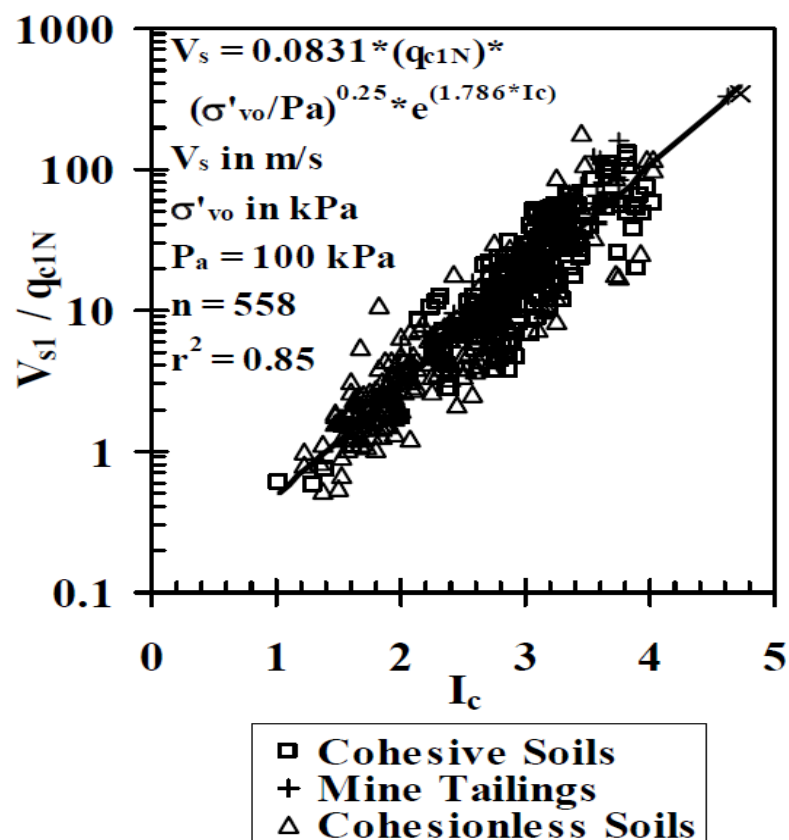
Figure 2. 6. Developed correlation as a function of I_c

(Source: Hegazy and Mayne, 2006)

Andrus et al. (2007) performed in situ tests and proposed correlations between V_{s1} and CPT for different geological ages. Correlations were proposed using 229 data. Of the 229 data, 143 were obtained from South Carolina, 80 from California, and 6 from Japan. The data belong to 3 different geological ages. 72 data are Holocene age, 113 data are Pleistocene age, and 44 data are tertiary age. Shear wave measurements were made using

SCPT for 209 data, test CHT for 14 data, and SL for 6 data. Figure 2.7 shows the comparison of measured and calculated V_{s1} using a proposed equation for Holocene age sand by Andrus et al. (2007).
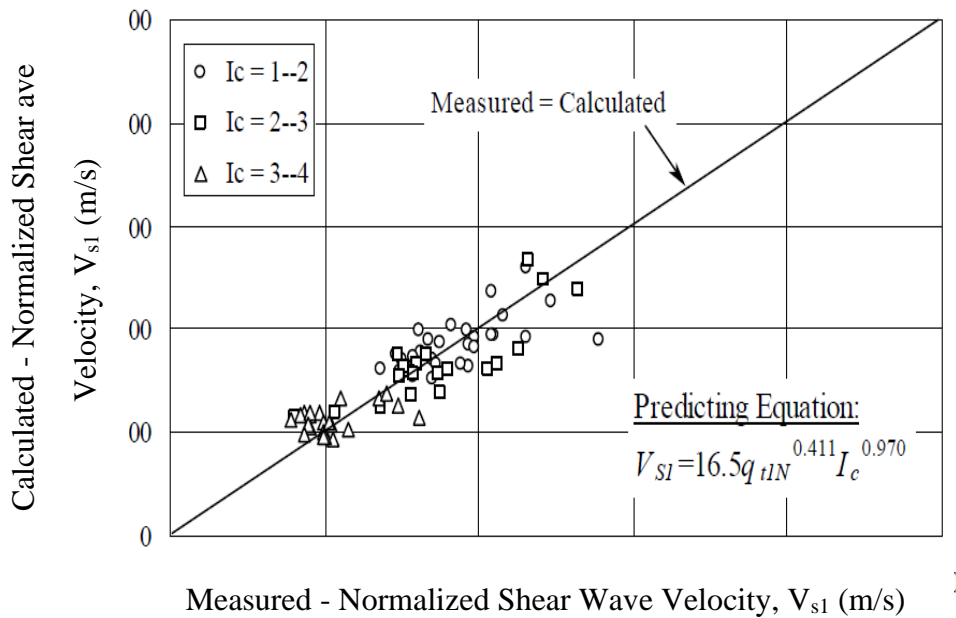
Figure 2. 7. Comparison of measured and calculated V_{s1} using predicting equation for the Holocene age sand (Source: Andrus et al., 2007)

Robertson (2009) developed the relationship between CPT and V_{s1} given in Table 2.2 using existing laboratory and field test results for all soil types. Studies were carried out on 1035 data obtained from Holocene and Pleistocene aged – uncemented silica soils.

Karray et al. (2011) studied more than 900 V_s profiles and proposed a relationship between CPT and V_{s1} for uncemented and Holocene age granular soils. 900 V_s profiles were obtained from the Péribonka site in Canada by performing in-situ tests. Shear wave measurements were made using modal analysis of surface waves (MASW). Figure 2.8 shows the V_{s1} as a function of q_{c1} for the Peribonka site by Karray et al. (2011).
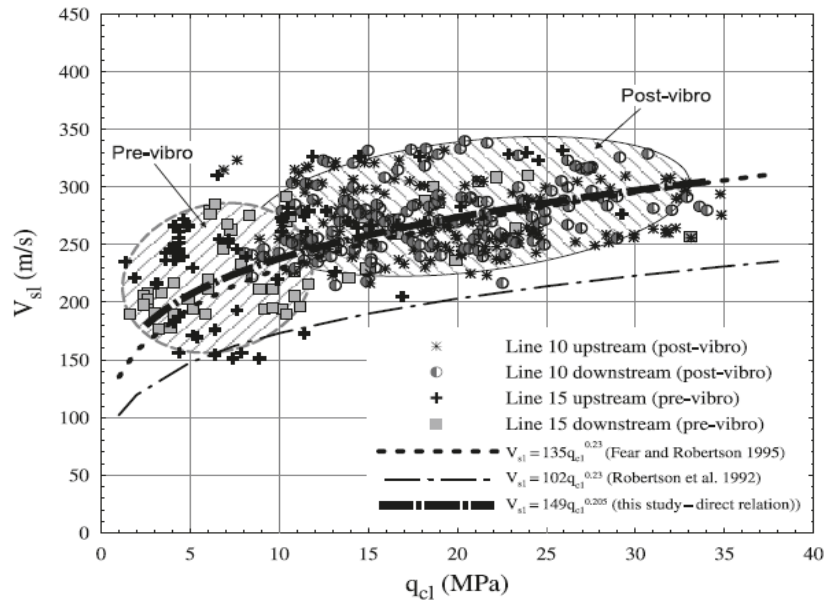
Figure 2. 8. V_{s1} as a function of q_{c1} for Peribonka site

(Source: Karray et al., 2011)

Cai et al. (2014) proposed a correlation for clay deposits between CPT and V_{s1} using in-situ test results. The test results were obtained from 7 sites in the Jiangsu Province of eastern China. Shear wave measurements were made using SCPT, cross-hole test CHT, downhole DHT test, and spectral analysis surface wave SASW. Figure 2.9 shows the V_{s1} as a function of q_{c1} for Jiangsu clays by Cai et al. (2007).
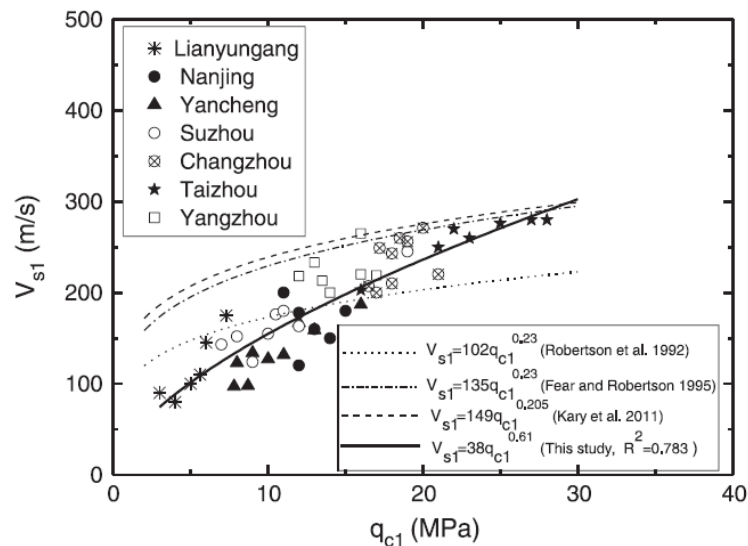
Figure 2. 9. V_{s1} as a function of q_{c1} for Jiangsu clays

(Source: Cai et al., 2007)

Ecemis (2020) studied 115 data and proposed a soil type index dependent relationship between CPT and V_{s1} for Holocene age – unbounded soils. 115 data were obtained from 13 sites on the northern coast of Izmir Gulf by performing in-situ tests. Shear wave measurements were made using SCPT. Figure 2.10 shows the proposed relationship between V_{s1} and q_{c1N} for Holocene-age, unbounded soils by Ecemis (2020).
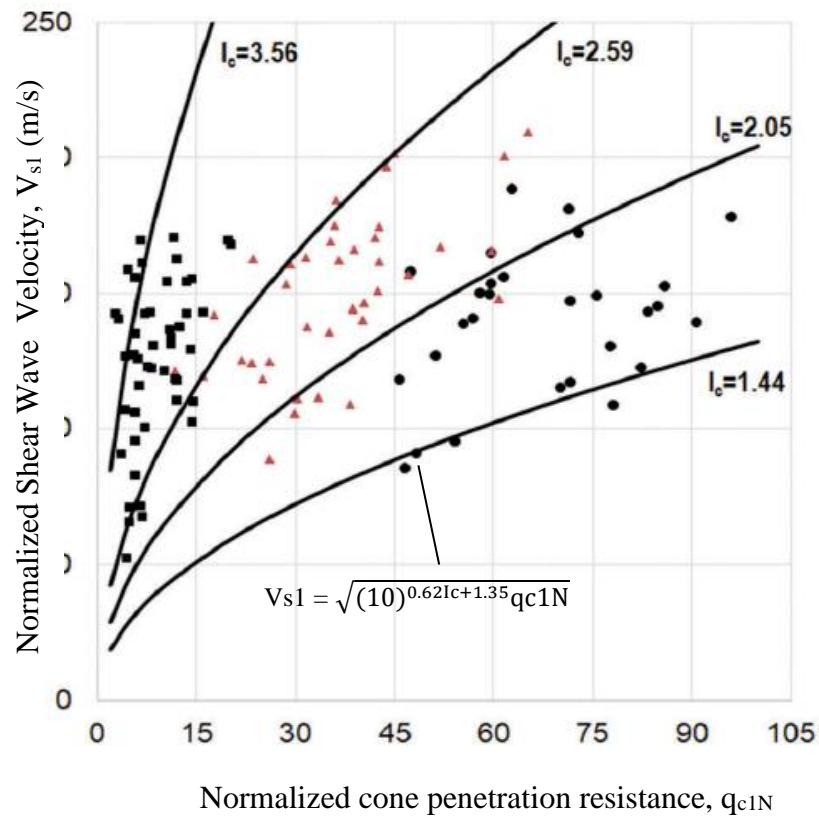
Figure 2. 10. Variation of V_{s1} with q_{c1N} for Holocene-age, unbounded soils
(Source: Ecemis, 2020).

Many researchers have developed correlations between V_{s1} and q_{c1N} to facilitate the analysis of the complex structure of soils. The researchers used the data they obtained by performing laboratory or field tests while developing their correlations. They used only one soil type in their experiments and did not use soils with different fines content (FC). Correlations have been developed for sands or clays; there are not enough studies for soils with different FC.

Shear wave measurements were made using SCPT, CHT, DHT, SASW, SL, MASW, and resonant column tests in the existing researchs. Except for Baldi et al. (1989) and Rix and Stokoe (1991), shear wave measurements were not made in the laboratory. Baldi et al. (1989) and Rix and Stokoe (1991) measured shear wave velocity by applying the resonant column test. In other studies, (e.g., Robertson et al., 1992; Hegazy and Mayne, 1995; Fear and Robertson, 1995; Mayne and Rix, 1995; (Andrus et al., 2004; Hegazy and Mayne, 2006; Andrus et al., 2007; Robertson, 2009; Karray et al., 2011; Cai et al., 2014; Ecemis 2020) shear wave measurements were found by performing in-situ tests.

Two different correlation equations have been developed by the researchers, the soil type dependent correlation equations and the equations for different soil types. Hegazy and Mayne (2006), Andrus et al. (2007), Robertson (2009), and Ecemis (2020) developed correlations based on soil type index (I_c).

CHAPTER 3

PREPARATION AND PROPERTIES OF THE SAMPLES

3.1. Introduction

This chapter describes the soil box, the preparation of the samples used in the experiments, and the sample properties. The experiments were carried out inside the aluminum box with a wheeled platform. The box had rigid side boundaries. A total of 12 soil samples were prepared with silty sands containing 0% (clean sand), 5%, 15%, and 35% silt by weight.

Three different experiments were carried out for each loose, medium dense, and dense soil sample. Mixing the sand and silt and filling processes were performed before the experiments. Mixing processes were carried out to prepare homogeneous 5%, 15%, and 35% silty sands. Sample filling operations were done inside the box with the buckets, and precision scales were used.

3.2. Soil box

A soil box with a length of 160 cm, a depth of 100 cm, and a width of 40 cm was used in the experiments. As shown in Figure 3.1, the box is adjusted to the height used in the experiments. The box is fixed from the sides, and six wheels are placed to the base of the box to move it from one place to another. A 1mm thick membrane was placed inside the laminar box to prevent water leakage and soil movement. In this study, the samples were dry.
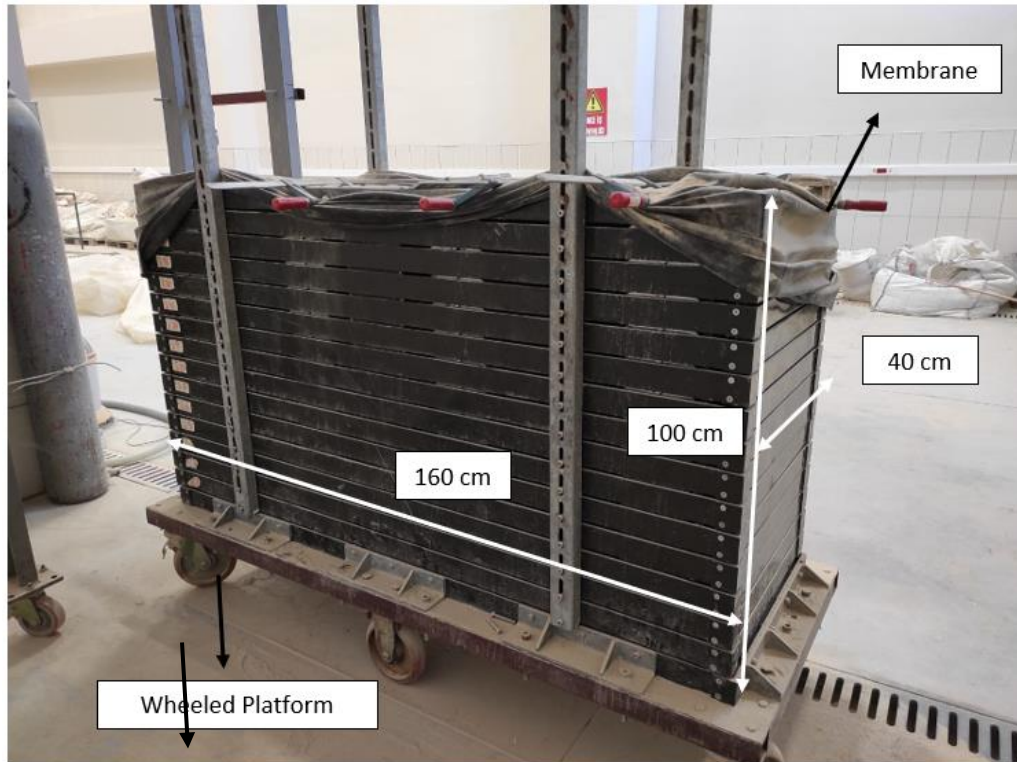
Figure 3.1. Soil box for experiments

3.3. Sample preparation for the experiments

Dry clean sand and silty sands containing 5%, 15%, and 35% silt by weight were used in the experiments. Soil mixing was done in a 150 cm length and 75 cm wide box according to the sand to silt ratio. Three different soil samples (loose, medium dense, and dense) were prepared before each experiment with varying ratios of silt.

After the mixing and preparation phases were completed, the samples were filled into the soil box layer by layer using metal buckets. The densification process has been applied to the layers. While the densification process was not applied to loose soils, it was applied to medium and dense soils. A densification plate was used for this process. The plate was applied (compacted) to the soil layers once for medium dense soil. The same process was applied (compacted) to each layer twice for dense soil. The measurement of the sample weights in the buckets was made with the help of precision scales.

The reason for filling the samples layer by layer is to obtain a homogeneous sample. Figures show the change of soil height by time during the filling process. S1 represents the soil sample number. Figures 3.2 to 3.5 show the total sample weights used in the experiments and the time spent. These figures also show the soil layers created.

Figure 3.2.(a) shows the preparation of clean loose sand for the experiment. During the filling operations, nine soil layers were formed. The height of the sand in the box after each layer is created is also seen in the figure. In the preparation of clean loose sand, first 103.1 kg of clean sand was filled into the box, then a total of 877.8 kg of clean sand was filled into the box.

Figure 3.2.(b) shows the preparation of clean medium dense sand for the experiment. During the filling operations, nine soil layers were formed. The height of the sand in the box after each layer is created is also seen in the figure. In the preparation of clean medium dense sand, first 102.2 kg of clean sand was filled into the box, then a total of 916 kg of clean sand was filled into the box.

Figure 3.2.(c) shows the preparation of clean, dense sand for the experiment. During the filling operations, six soil layers were formed. The height of the sand in the box after each layer is created is also seen in the figure. In the preparation of clean, dense sand, first 158.2 kg of clean sand was filled into the box, then a total of 952.1 kg of clean sand was filled into the box.
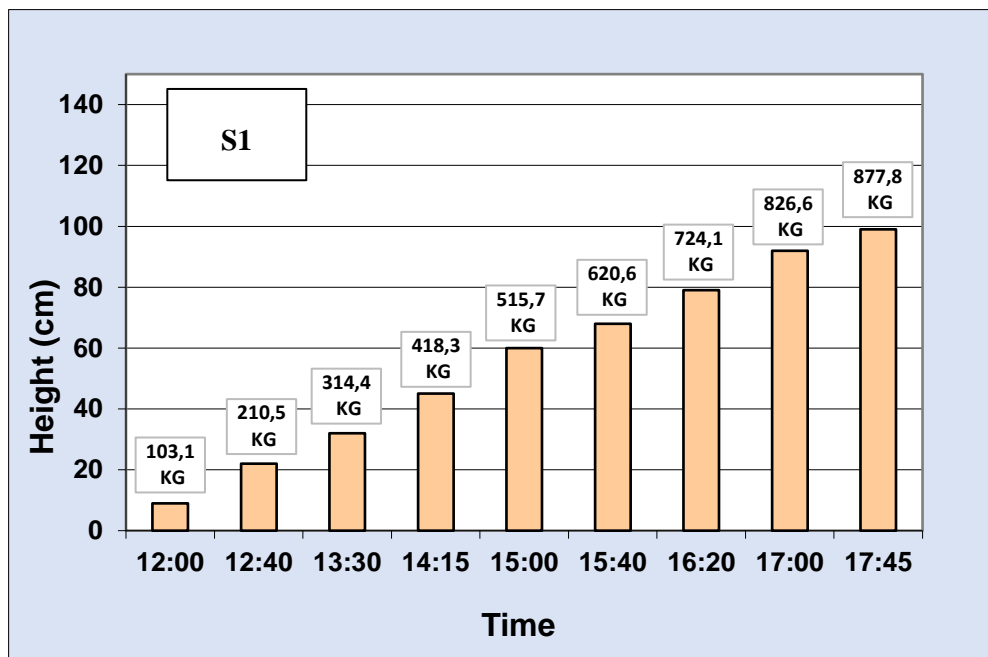
(a)

Figure 3.2. Preparation of clean sand (0% silt) and soil layers for (a) loose, (b) medium dense, (c) dense sand

(b)
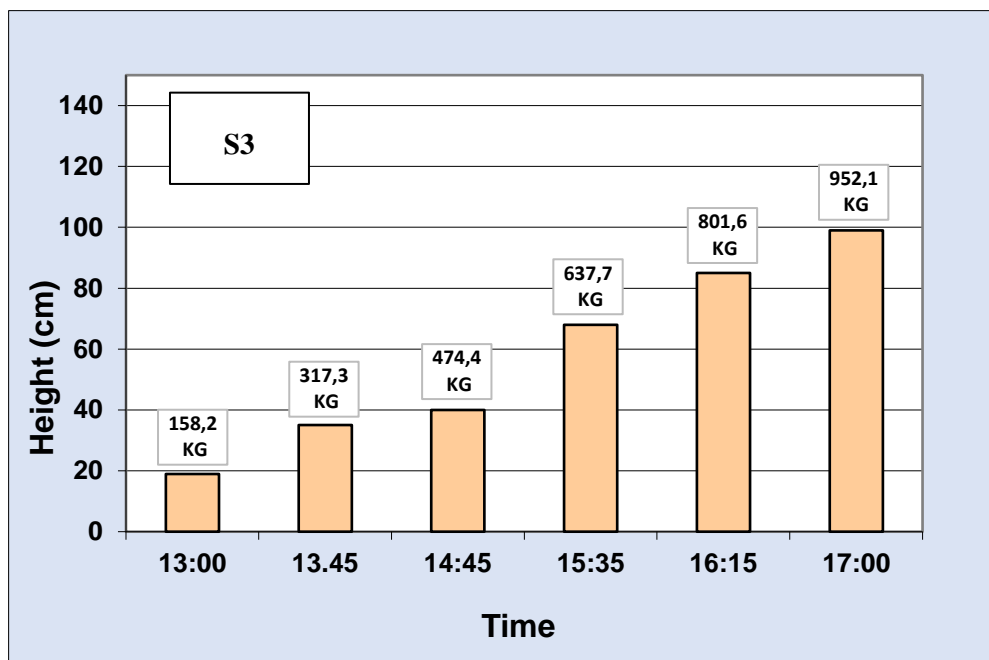
(c)

Figure 3.2 (cont.)

Figure 3.3.(a) shows the preparation of 5% silty loose sand for the experiment. Six soil layers were formed during the filling operations. The height of the sand in the box after each layer is created is also seen in the figure. In the preparation of 5% silty

loose sand, the first 162.9 kg of 5% silty sand was filled into the box, then a total of 904.7 kg of 5% silty sand was filled into the box.

Figure 3.3.(b) shows the preparation of 5% silty medium dense sand for the experiment. Six soil layers were formed during the filling operations. The height of the sand in the box after each layer is created is also seen in the figure. In the preparation of 5% silty medium dense sand, the first 166.8 kg of 5% silty sand was filled into the box, then a total of 930.6 kg of 5% silty sand was filled into the box.

Figure 3.3.(c) shows the preparation of 5% silty dense sand for the experiment. Six soil layers were formed during the filling operations. The height of the sand in the box after each layer is created is also seen in the figure. In the preparation of 5% silty dense sand, the first 161.1 kg of 5% silty sand was filled into the box, then a total of 959 kg of 5% silty sand was filled into the box.

(a)

Figure 3.3. Preparation of 5% silty sand and soil layers for (a) loose, (b) medium dense, (c) dense sand
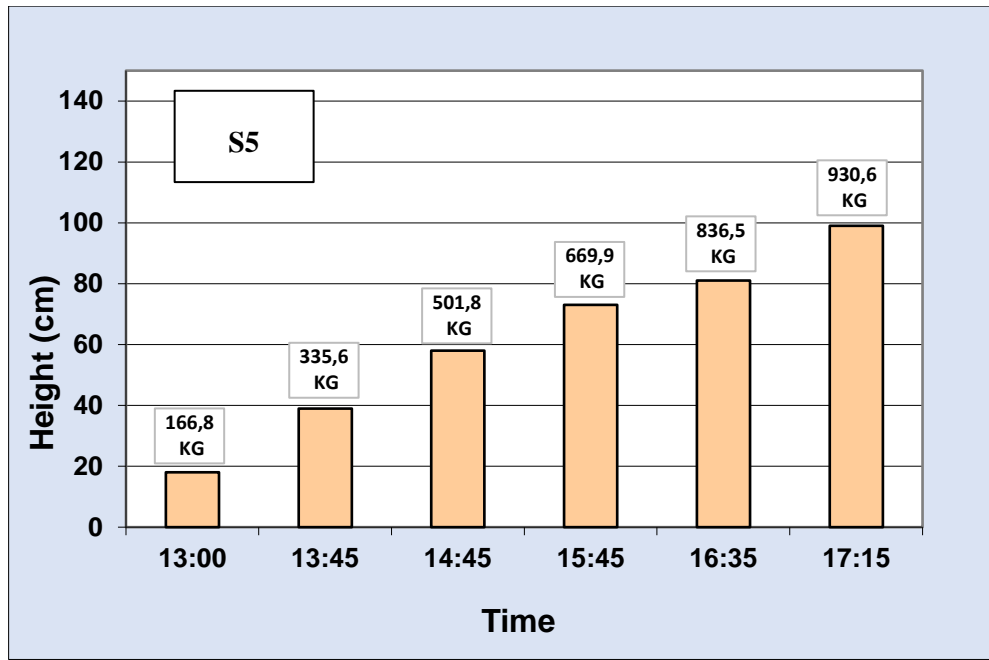
(b)
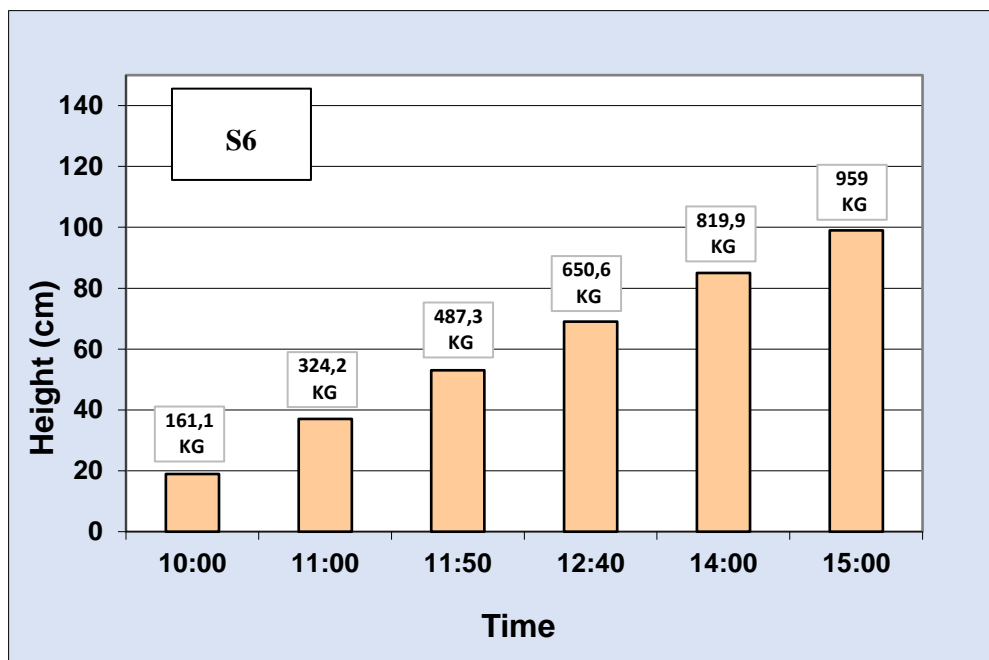
(c)

Figure 3.3 (cont.)

Figure 3.4.(a) shows the preparation of 15% silty loose sand for the experiment. During the filling operations, eight soil layers were formed. The height of the sand in the box after each layer is created is also seen in the figure. In the preparation of 15% silty

loose sand, the first 114.1 kg of 15% silty was filled into the box, then a total of 936.1 kg of 15% silty sand was filled into the box.

Figure 3.4.(b) shows the preparation of 15% silty medium dense sand for the experiment. Six soil layers were formed during the filling operations. The height of the sand in the box after each layer is created is also seen in the figure. In the preparation of 15% silty medium dense sand, the first 167.9 kg of 15% silty was filled into the box, then a total of 978.6 kg of 15% silty sand was filled into the box.

Figure 3.4.(c) shows the preparation of 15% silty dense sand for the experiment. During the filling operations, soil layers were formed. The height of the sand in the box after each layer is created is also seen in the figure. In the preparation of 15% silty dense sand, first 170.2 kg of 15% silty was filled into the box, then a total of 1020 kg of 15% silty sand was filled into the box.
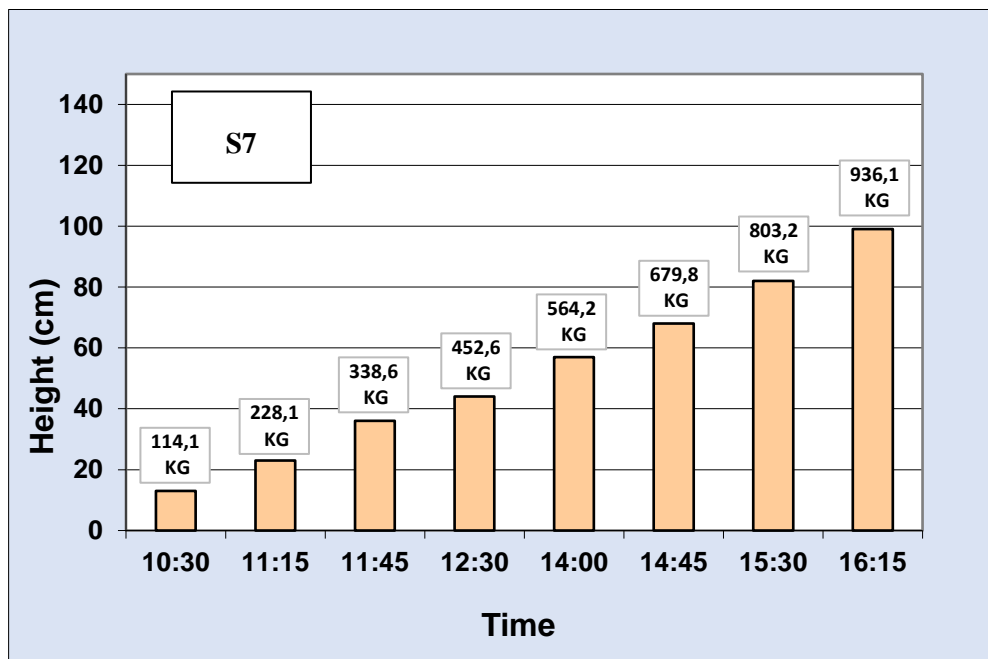
(a)

Figure 3.4. Preparation of 15% silty sand and soil layers for (a) loose, (b) medium dense, (c) dense sand

(cont. on next page)
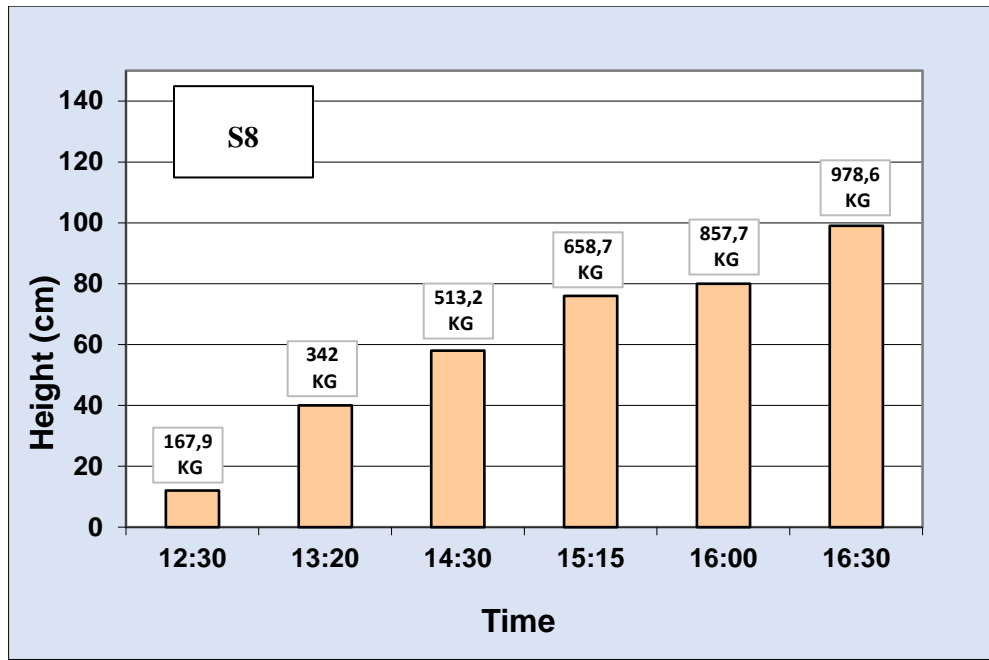
(b)
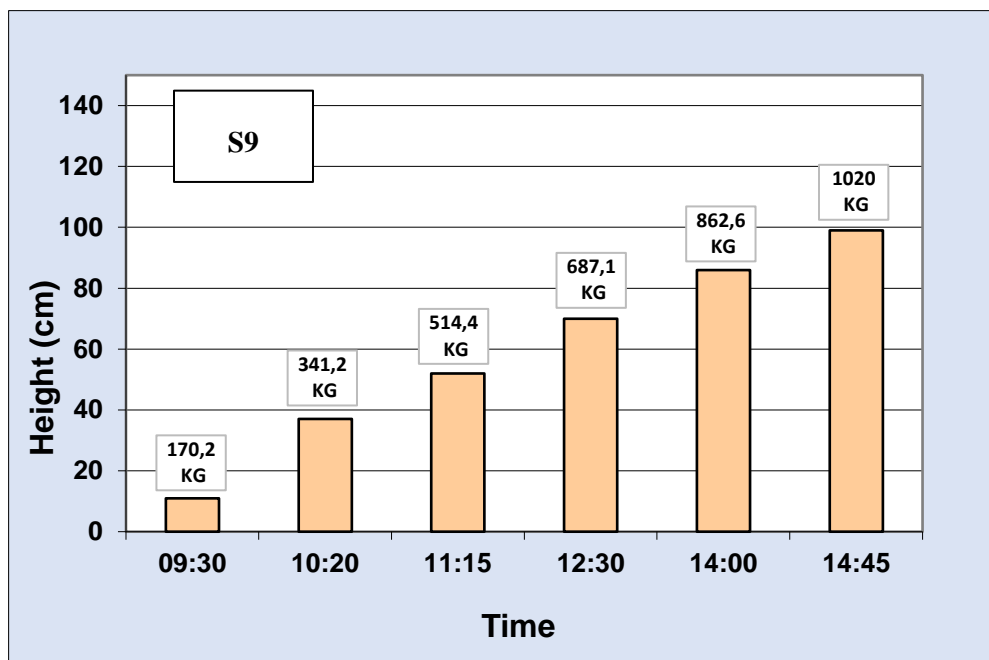
(c)

Figure 3.4 (cont.)

Figure 3.5.(a) shows the preparation of 35% silty loose sand for the experiment. During the filling operations, nine soil layers were formed. The height of the sand in the box after each layer is created is also seen in the figure. In the preparation of 35% silty

loose sand, 105.8 kg of 35% silty sand was first filled into the box, then a total of 1000 kg of 35% silty sand was filled into the box.
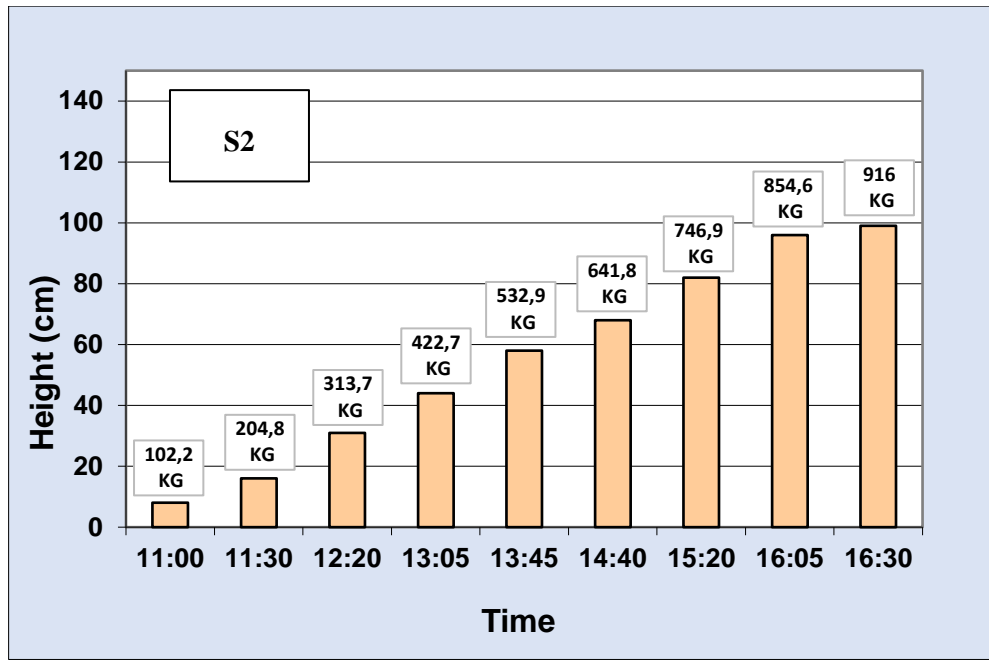
Figure 3.5.(b) shows the preparation of 35% silty medium dense sand for the experiment. During the filling operations, nine soil layers were formed. The height of the sand in the box after each layer is created is also seen in the figure. In the preparation of 35% silty medium dense sand, first 120.2 kg of 35% silty sand was filled into the box, then a total of 1068.2 kg of 35% silty sand was filled into the box.

Figure 3.5.(c) shows the preparation of 35% silty dense sand for the experiment. Ten soil layers were formed during the filling operations. The height of the sand in the box after each layer is created is also seen in the figure. In the preparation of 35% silty dense sand, first 109.7 kg of 35% silty sand was filled into the box, then a total of 1108 kg of 35% silty sand was filled into the box.
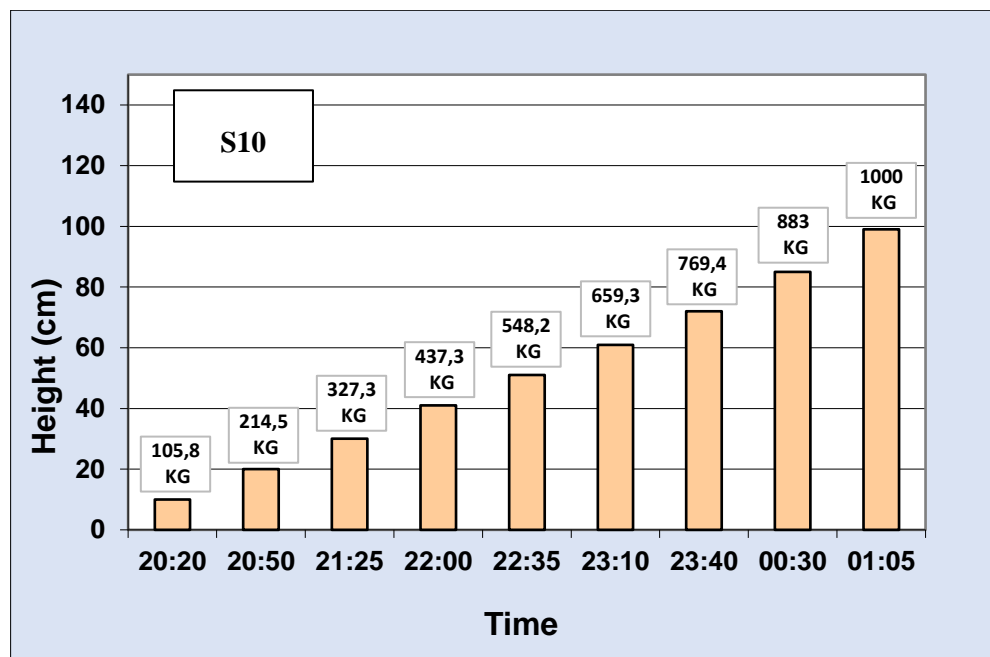

(a)

Figure 3.5. Preparation of 35% silty sand and soil layers for (a) loose, (b) medium dense, (c) dense sand
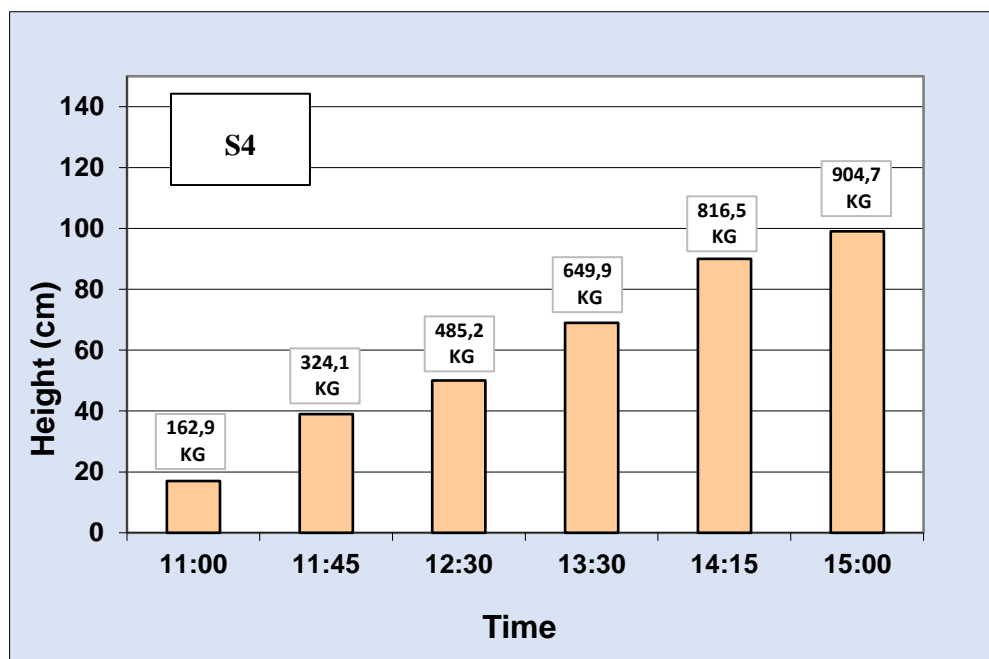
(cont. on next page)
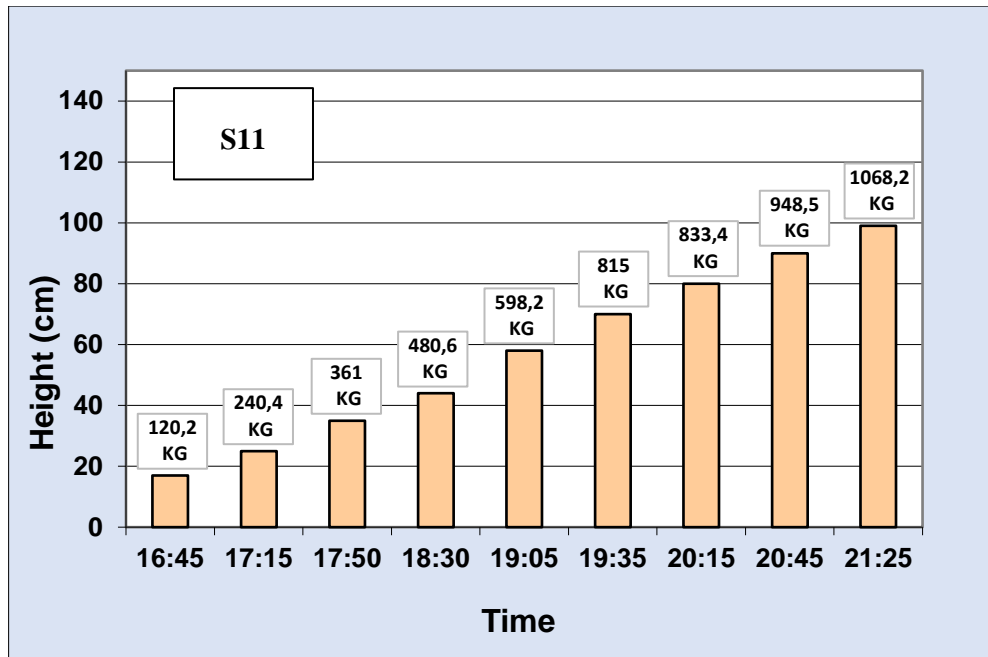
(b)
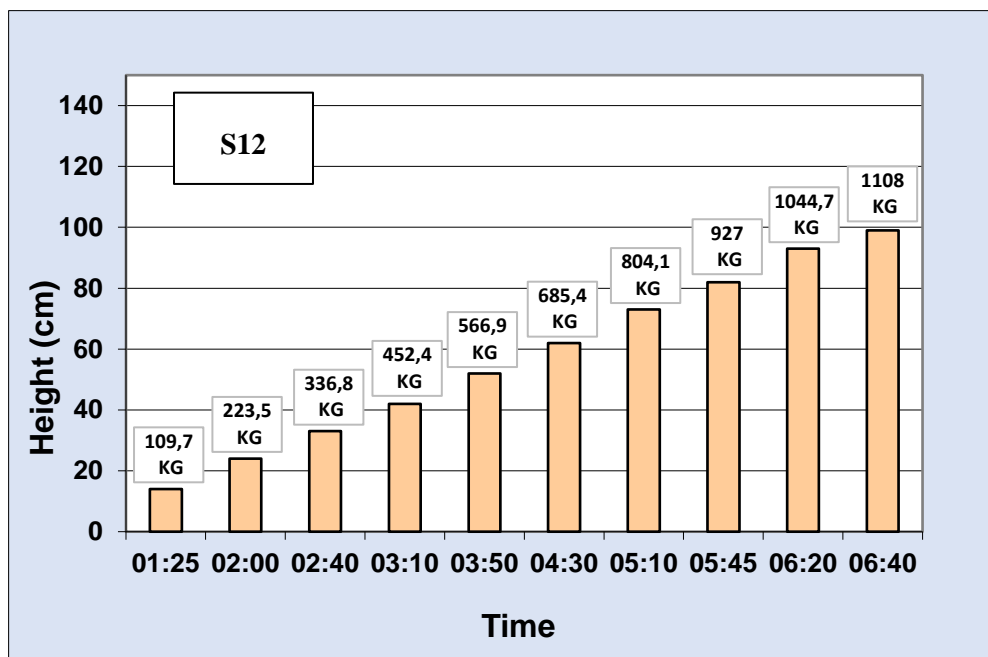
(c)

Figure 3.5 (cont.)

Table 3.1 shows the total weight and density of the clean sand (0% silt), 5% silty sand, 15% silty sand, and 35% silty sand samples prepared inside the box. The total volume of the box is 0.63 m³ which is same in all experiments. The calculations for sample density are explained in detail under the title of sample properties.

Table 3.1. Total weight and unit weight of soil samples used in the experiment.

Sample No	FC	Total weight of prepared Soil Samples (W)	Unit weight (γ)
-	(%)	(kg)	(kN/m³)
S1	0	877.8	13.59
S2		916	14.18
S3		952.1	14.74
S4	5	904.7	14.01
S5		930.6	14.41
S6		959	14.85
S7	15	936.1	14.49
S8		978.6	15.15
S9		1020	15.79
S10	35	1000	15.48
S11		1068	16.54
S12		1108	17.16

As seen in Table 3.1, the total dense soils' weight used in the box is more than the total weight of the loose soils used in the box. This indicated an increase in solid particles in the same volume and the increase in relative density.

3.4. Sample Properties

Table 3.2 shows the physical properties of the clean sand and silty sand used in the experiments. The maximum void ratio (e_{max}), minimum void ratio (e_{min}) and specific gravity (G_s) were obtained from Ecemis et al. (2022).

Table 3.2. Properties of soil samples used in the experiment (Ecemis et al. 2022)

Type of soil	FC (%)	e_{max}	e_{min}	G_s
Clean sand	0	1	0.72	2.64
Silty sand	5	0.94	0.68	2.64
	15	0.88	0.58	2.65
	35	0.83	0.43	2.66

Relative density (D_r) was calculated using the information in Table 3.2. D_r and void ratio (e) are calculated by the equations given below;

$$\frac{e_{max} - e}{e_{max} - e_{min}} \tag{3.1}$$

$$e = \frac{\text{Volume of Voids}}{\text{Volume of Soil Solids}} = \frac{\text{Total volume} - \text{Volume of Soil Solids}}{\text{Volume of Soil Solids}} \tag{3.2}$$

The total volume is calculated using the dimensions of the box. The box is 160 cm in length, 100 cm in depth, and 40 cm wide. During the filling processes before the experiments, the soil box was filled with dry soil from the bottom to the top. Hence the main parameter that determines the box's volume is the height of the soil sample inside the box. After each soil preparation, an opening of 1 cm is left at the top of the box. Total volume is calculated by using the equation below;

$$\text{Total Volume} = \text{Length of Box} * \text{Width of Box} * \text{Height of the Soil Sample} \tag{3.3}$$

The only unknown in equation 3.1 is the volume of the soil solids. The volume of soil solids is calculated by equation 3.4. The unit weight of the sample is calculated by equation 3.5.

$$\text{Volume of Soil Solids} = \frac{\text{Weight of soil solids}}{\text{Gs} * \text{Unit Weight of Water}} \tag{3.4}$$

$$\text{Unit Weight} = \frac{\text{Weight of soil solids}}{\text{Total volume}} \tag{3.5}$$

Total volume, the weight of soil solids, volume of soil solids, unit weight, void ratio, and relative density of clean sand (0% silt), 5% silty sand, 15% silty sand, 35% silty sand for loose, medium dense, and dense states are shown in Tables 3.3 to 3.6.

Table 3.3. Total volume, the weight of soil solids, volume of soil solids, unit weight, (e) and (D$_r$) of clean sand (0% silt) for loose, medium dense, and dense states

Sample No	FC	Total Volume	Weight of Soil Solids	Volume of Soil Solids	Unit Weight	Void Ratio (e)	Relative Density (D$_r$)
-	(%)	(m^3)	(kg)	(m^3)	(kN/m^3)	-	%
S1			877.8	0.33	13.59	0.91	34
S2	0	0.63	916	0.35	14.18	0.83	62
S3			952.1	0.36	14.74	0.76	87

Table 3.4. Total volume, the weight of soil solids, volume of soil solids, unit weight, (e) and (D$_r$) of 5% silty sand for loose, medium dense, and dense states

Sample No	FC	Total Volume	Weight of Soil Solids	Volume of Soil Solids	Unit Weight	Void Ratio (e)	Relative Density (D$_r$)
-	(%)	(m^3)	(kg)	(m^3)	(kN/m^3)	-	%
S4			904.7	0.34	14.01	0.85	35
S5	5	0.63	930.6	0.35	14.41	0.80	55
S6			959	0.36	14.85	0.74	75

Table 3.5. Total volume, weight of soil solids, volume of soil solids, unit weight, (e) and (D$_r$) of 15% silty sand for loose, medium dense and dense states

Sample No	FC	Total Volume	Weight of Soil Solids	Volume of Soil Solids	Unit Weight	Void Ratio (e)	Relative Density (D$_r$)
-	(%)	(m^3)	(kg)	(m^3)	(kN/m^3)	-	%
S7			936.1	0.35	14.49	0.79	29
S8	15	0.63	978.6	0.37	15.15	0.72	55
S9			1020	0.38	15.79	0.65	78

Table 3.6. Total volume, weight of soil solids, volume of soil solids, unit weight, (e) and (D$_r$) of 35% silty sand for loose, medium dense and dense states

Sample No	FC	Total Volume	Weight of Soil Solids	Volume of Soil Solids	Unit Weight	Void Ratio (e)	Relative Density (D$_r$)
-	(%)	(m^3)	(kg)	(m^3)	(kN/m^3)	-	%
S10			1000	0.38	15.48	0.69	36
S11	35	0.63	1068	0.40	16.54	0.58	63
S12			1108	0.42	17.16	0.52	77

CHAPTER 4

LABORATORY STUDY

4.1. Introduction

The seismic cone penetration tests (SCPT) were carried out in a controlled manner in İzmir Institude of Technology (IZTECH) geotechnical engineering laboratory. Laboratory experiments have certain advantages and disadvantages. The benefits of laboratory experiments are that they are controllable, easily reproducible, repeatable, and provide precise and accurate data. On the contrary, working with less massive and disturbed samples are disadvantage of laboratory experiments.

The SCPT experiments were carried out in a fixed 160 cm length, 100 cm depth, and 40 cm wide soil box. SCPT tests were applied to soils with four different silt ratios by weight. These are clean sand, 5% silty sand, 15% silty sand, and 35% silty sand. Experiments were carried out at three different relative densities for each soil sample. A total of 12 experiments were performed. Figure 4.1 shows the schematic view of SCPT experiments. Cone penetration was applied at 40 cm from the right side. Seismic experiments were carried out at a distance of 20 cm from the left side.

In this chapter, SCPT test equipment, and the test procedure is explained. From SCPT tests it is aimed to find q_c, and V_s of clean sand and silty sand at diffrent dense states prepared inside the box.
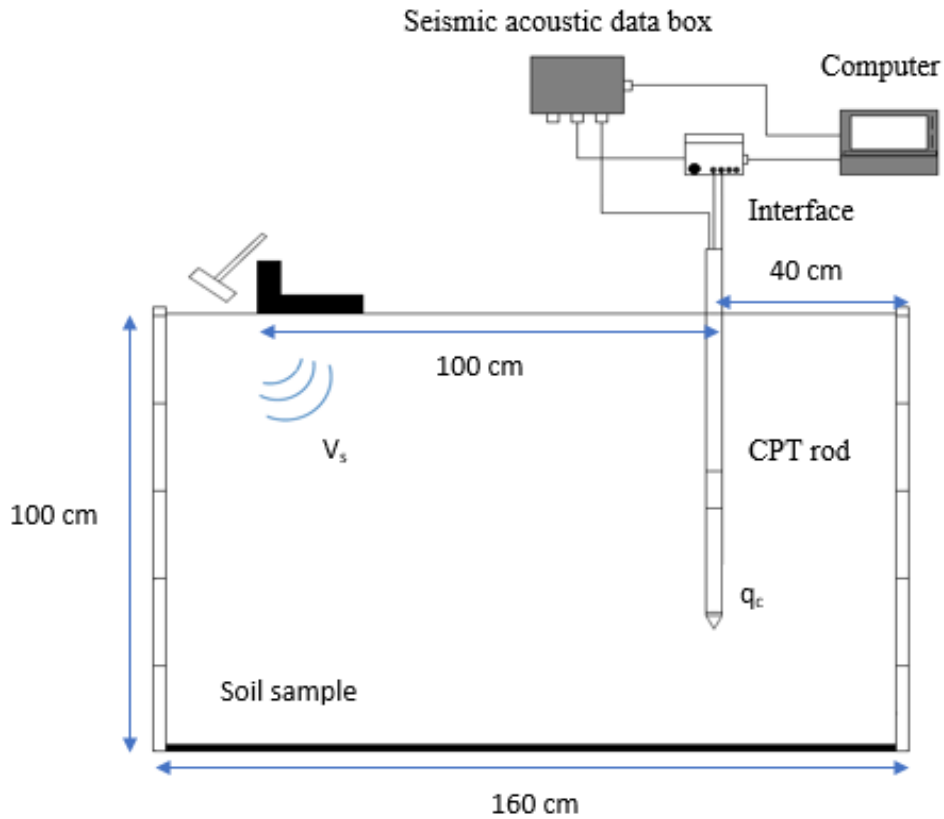
Figure 4.1. Schematic view of SCPT experiments

4.2. Seismic Cone Penetration Test (SCPT)

SCPT was obtained with the development of the cone penetration test (CPT). CPT is applied to a sample inside the soil box and is a practical test for determining soil parameters using a cylindrical cone that moves vertically through the ground at a constant velocity of 2cm/sec (ASTM D5778-12). As a result of CPT analysis, soil parameters such as q_c and f_s are obtained. The pore water pressure, which results from the cone penetrating the ground, can be measured using the CPTu. CPT has important advantages such as providing rapid, reliable and continuous data and being economical (Robertson, 2016). CPT is used to determine soil parameters, soil type, and content and provides data for better results in geotechnical design.

Seismic cone penetration test is actually the combination of the seismic downhole method and the CPT logging (Robertson et al., 1986). In the field, the down-hole and cross-hole methods are usually used for shear wave velocity (V_s) measurements. Generally, bender element (BE) tests are used in the laboratory for V_s measurements. This study used SCPT because it gives more precise results than the bender element test, and

31

the samples are in large masses. SCPT was carried out for clean and silty sands at different relative densities. This test uses seismic equipment in addition to the equipment used for the CPT test.

4.2.1. Test Equipment

Equipment from Geotech company were used in SCPT experiments. Test equipment used for seismic cone penetration tests are a soil box, seismic acoustic data system, a cylindrical cone, CPT rod, S-plate, hammer, and hydraulic pump. The soil box dimension is shown in Figure 4.2. The box is 160 cm long, 100 cm depth and 40 cm wide. Soil box is composed of aluminium frame. The cylindrical cone used in the experiment is called a probe. The probe consists of two parts, the pizecone, and the nova. Piezecone has a 60-degree angled conical tip. The probe is 36 mm in diameter and weighs approximately 1.3 kg. Data transfer is carried out with the cable in the probe. CPT rod with 81 cm long was added to the probe's tip to reach the targeted depths during the experiments. Piezecone, nova, probe, and CPT rod that are used in the experiments are shown in Figure 4.3.
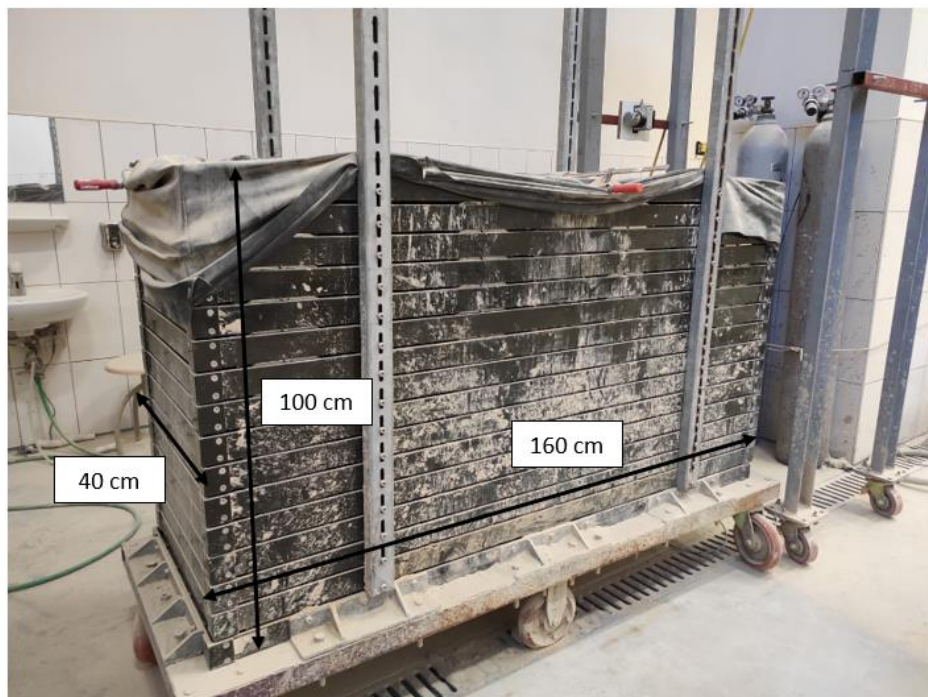
Figure 4.2. View of the soil box
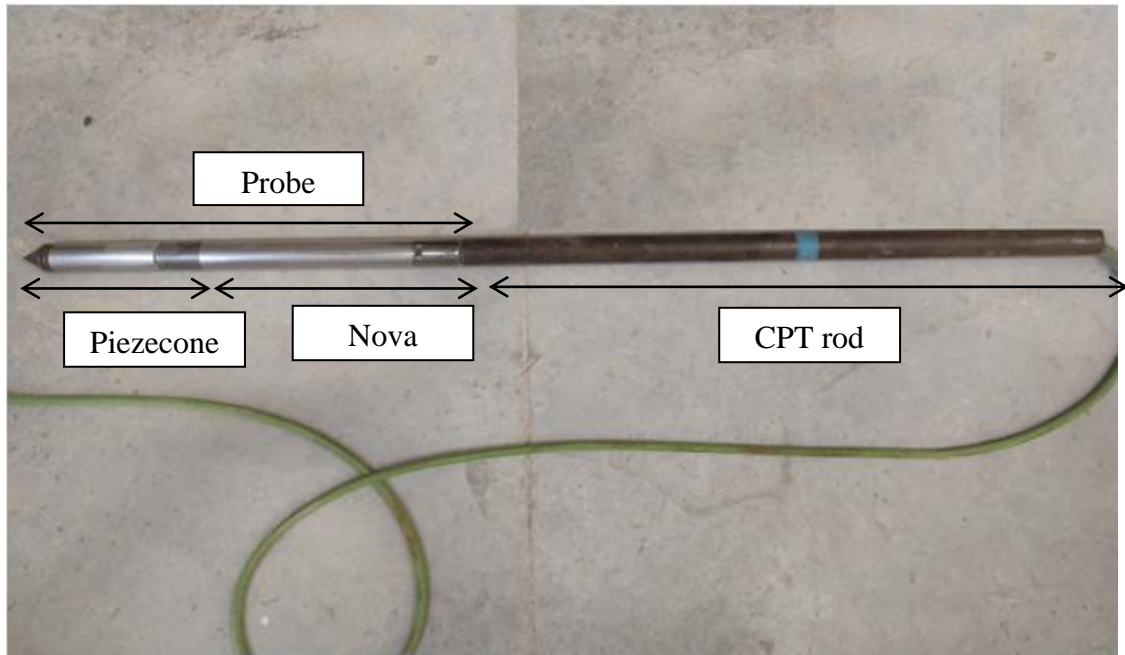
Figure 4.3. Piezecone, Nova, Probe and CPT rod

Probe, depth encoder, hammer, S-plate, interface, seismic acoustic data box, and computer form the seismic acoustic data system is shown in Figure 4.4. As the probe moves through the soil, the data reaches the computer interface through the cables inside the probe. At the same time, depth information is provided from the depth encoder. The data reaching the computer interface is displayed on the computer screen at the same time. CPT data comes from the interface and is displayed on the computer screen. These data are cone resistance (q_c) and friction resistance (f_s).

The penetration stops at 0.25m, 0.50m and 0.75 m depths to perform the seismic tests. Seismic cone penetration test experiments started with the hammer hitting the S-plate horizontally. Hammer and S-plate are called seismic equipment. Hammer and S-plate used in the experiments are shown in Figure 4.5. The triggered cable on the hammer is attached to the side of the S-plate. Shear waves were generated by horizontal hammer blows applied to the S-plate. The generated shear waves are detected by the seismic adapter connected to the probe and transmitted to the seismic acoustic data box via cables. The final signals are displayed on the computer screen.
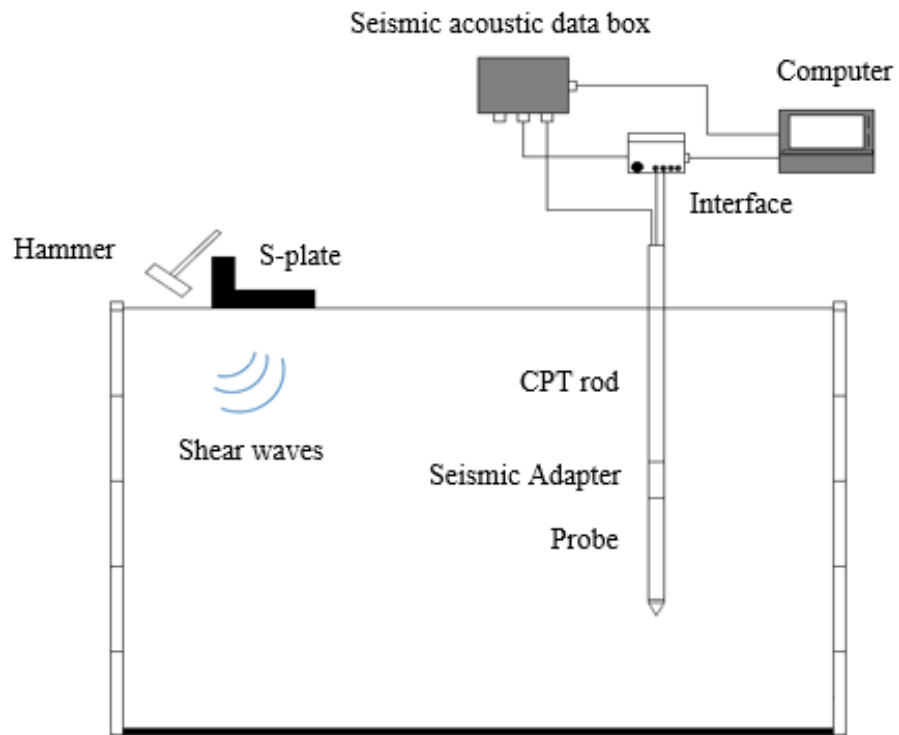
Figure 4.4. SCPT data system

(a)   (b)

Figure 4.5 (a) S-plate, (b) Hammer

A hydraulic pump is used to push the probe and CPT rod into the soil (Figure 4.6). The hydraulic pump pushed the probe and the CPT rod into the soil at approximately 0.75 m depth. The probe and CPT rod penetrated to the soil at a speed of between 1 cm and 1.5 cm per second. The hydraulic pump was stopped and moved at the depths where shear wave measurements were to be made using the remote control.

Figure 4.6. Hydraulic Pump

4.2.2. Test Procedure

Before the experiments, the hydraulic pump was brought to the position where the experiment was to be carried out and fixed to prevent its movement during the experiment. The depth encoder was connected with interface. CPT rod and probe were

combined. 0.4 m from the right side of the box surface was chosen as the starting point for probe penetration. After the test equipment was ready for the experiment, a zero test was applied to ensure that the system was working without any errors. Investigations begin with pushing the CPT probe to the soil with a hydraulic pump. The probe is penetrated up to the shear wave velocity testing depths. In the experiments, shear wave measurements were made at three different depths; 0.25m, 0.50m, and 0.75m. The CPT probe was stopped at these depths, and shear waves were generated using the hammer and S-plate. The S-plate was placed on the left side of the box with a distance of 1 meter from the probe. Shear waves were generated by hitting the S-plate with a hammer. Seismic cone penetration test experiments were performed on four different soils: clean sand, 5% silty sand, 15% silty sand, and 35% silty sand. Three experiments were performed for each soil sample as loose, medium dense, and dense states. A total of 12 SCPT tests were performed. Figure 4.7 shows the SCPT experiments performed in the laboratory.
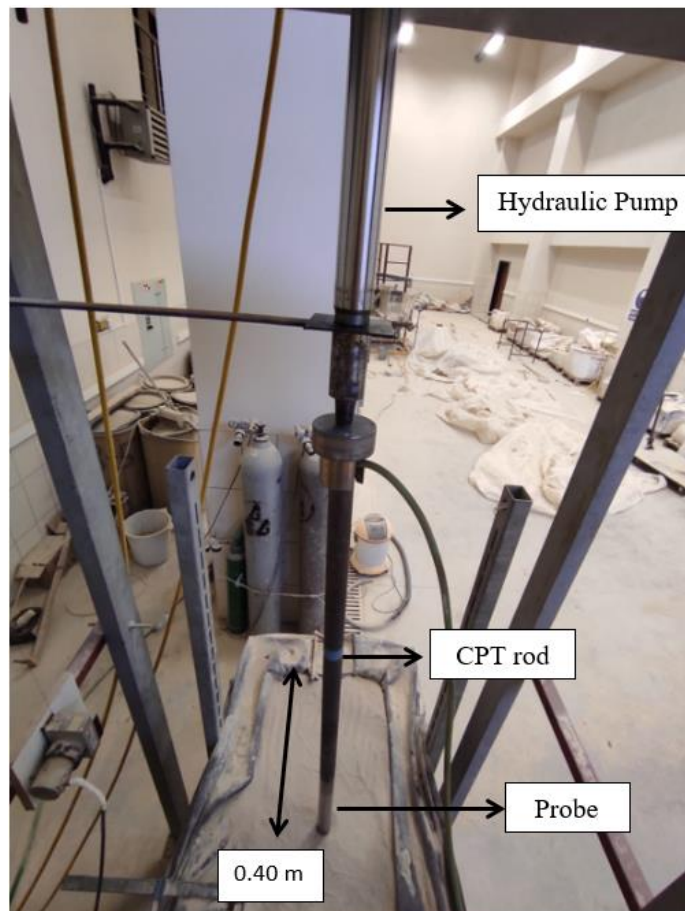
(a)
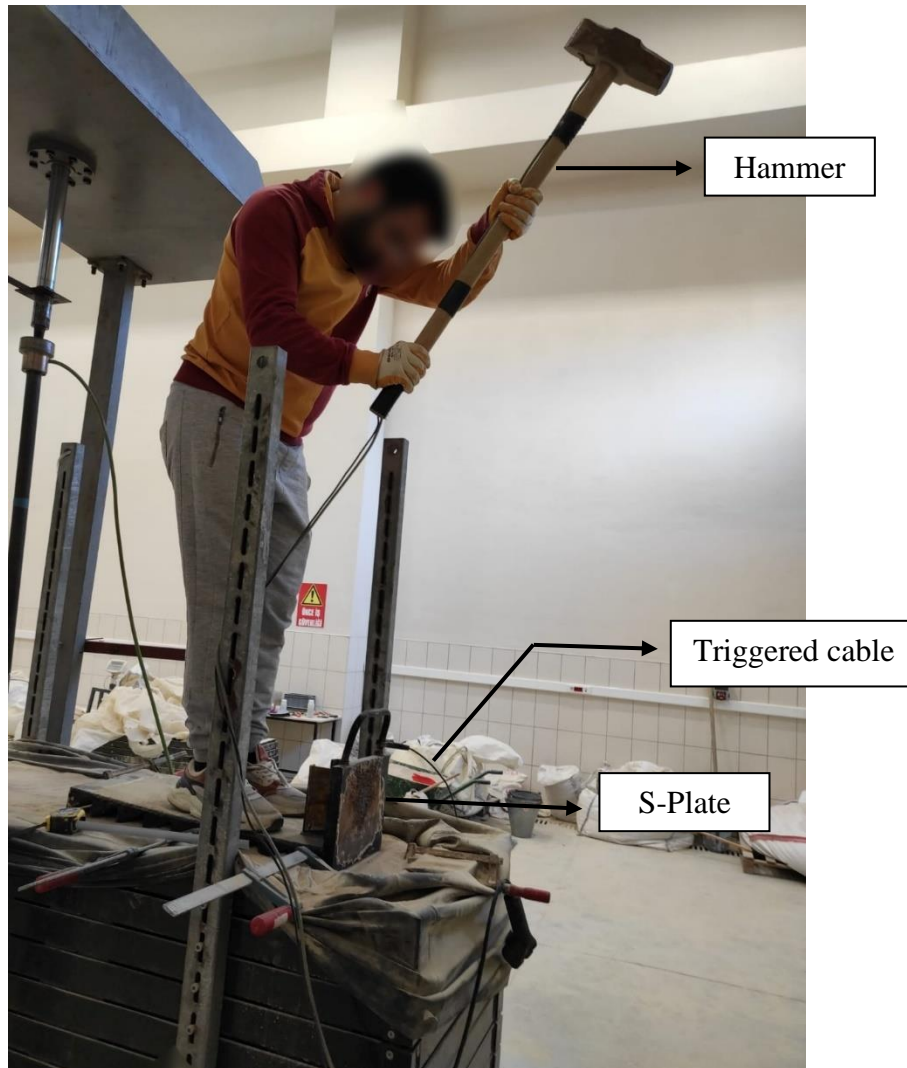
(b)

Figure 4.7 (a) Cone penetration (b) Seismic experiments

CHAPTER 5

LABORATORY TEST RESULTS

5.1. Introduction

In this chapter, the results of the SCPT test for clean sand, 5% silty sand, 15% silty sand, and 35% silty sand at different relative densities are presented. First, cone penetration resistance values obtained as a result of CPT experiments were given in detail. Then soil type index (I_c) values developed by Robertson and Wride (1998) were calculated using CPT data. The effect of relative density on q_c and I_c was shown on clean and silty sand.

The shear wave velocity data obtained from SCPT. Shear wave calculations were made using the cross-correlation method. The influence of soil type on q_c - V_s correlation was investigated with all data obtained from SCPT. A relationship between q_c and V_s based on soil type index has been proposed. Finally, the proposed relationship is compared with other available studies.

5.2. Cone penetration resistance

Cone penetration was performed to determine the q_c and f_s. Figure 5.1 shows the cone penetration resistance data of the CPT experiments applied to clean sand, 5% silty soil, 15% silty soil, and 35% silty soil at different relative densities. As a result of the experiments applied to four different soil samples, 12 CPT profiles were obtained, and the cone penetration resistance values were found between 0.1 MPa and 2 MPa.

Figure 5.1 (a) shows the cone resistance data by the depth for FC of 0% (clean sand). The figure shows the soil with three different relative densities as 34%, 62%, and %87. The relative density of sample 1 (S1) is 34%, and the average cone resistance is 0.25 MPa. The relative density of sample 2 (S2) is 62%, and average cone resistance is 0.72 MPa. The relative density of sample 3 (S3) is 87%, and average cone resistance is 1.17 MPa.

Figure 5.1 (b). shows the cone resistance by the depth for FC=5%. The figure shows the soil with three different relative densities as 35%, 55% and %75. The relative density of sample 4 (S4) is 35%, and the average cone resistance is 0.25 MPa. The relative density of sample 5 (S5) is 55% and average cone resistance is 0.67 MPa. The relative density of sample 6 (S6) is 75% and average cone resistance is 1.16 MPa.

Figure 5.1 (c). shows the cone resistance data by the depth for FC=15%. The figure shows the soil with three different relative densities as 29%, 55% and %78. The relative density of sample 7 (S7) is 29%, and the average cone resistance is 0.2 MPa. The relative density of sample 8 (S8) is 55%, and average cone resistance is 0.64 MPa. The relative density of sample 9 (S9) is 78%, and average cone resistance is 0.97 MPa.

Figure 5.1 (d). shows the cone resistance data by the depth for FC=35%. The figure shows the soil with three different relative densities as 36%, 63% and %77. The relative density of sample 10 (S10) is 36%, and the average cone resistance is 0.2 MPa. The relative density of sample 11 (S11) is 63%, and the average cone resistance is 0.45 MPa. The relative density of sample 12 (S12) is 77%, and average cone resistance is 0.94 Mpa.

Cone penetration resistance (q_c) increased throughout depth. The q_c for clean sand and silty sands is between 0.2 Mpa and 0.25 MPa at loose states, between 0.45 Mpa and 0.72 Mpa at medium dense states, and between 0.94 MPa and 1.17 MPa at dense states. In general, q_c increased as the relative density increased for each experiment with different FC. Also, q_c decreases as the FC increases.

(a)   (b)

(c)   (d)
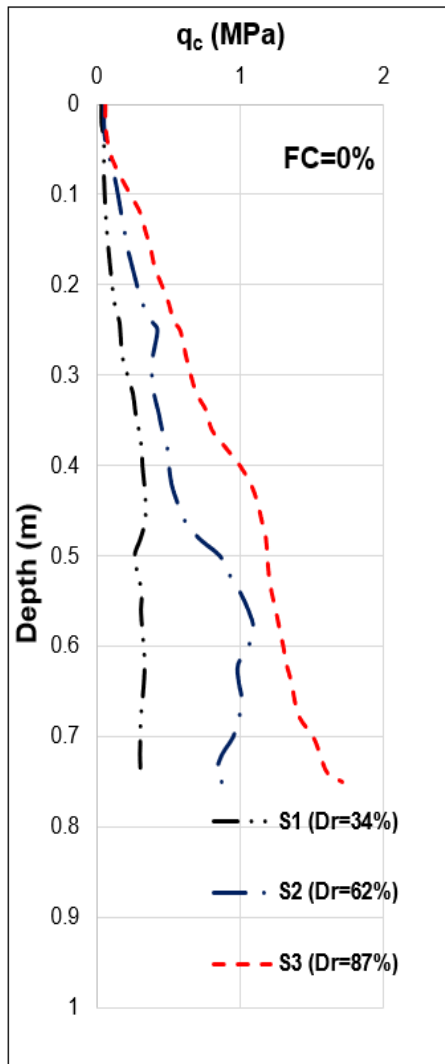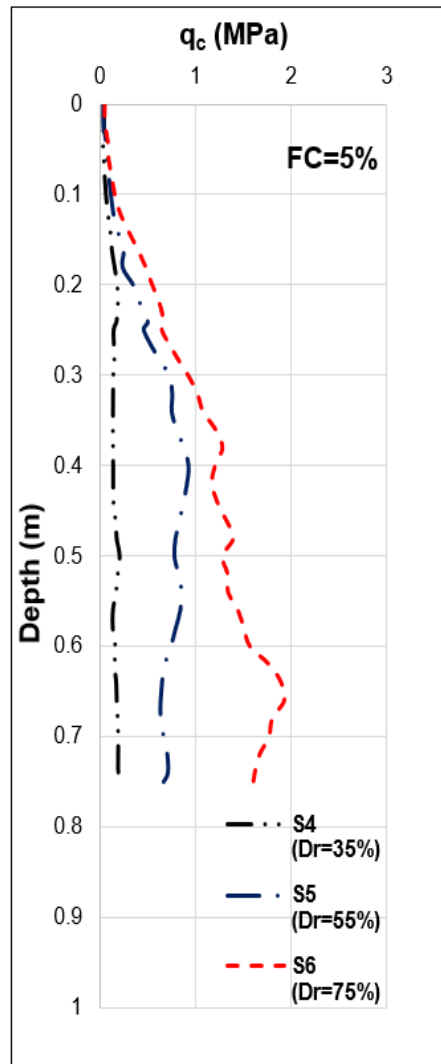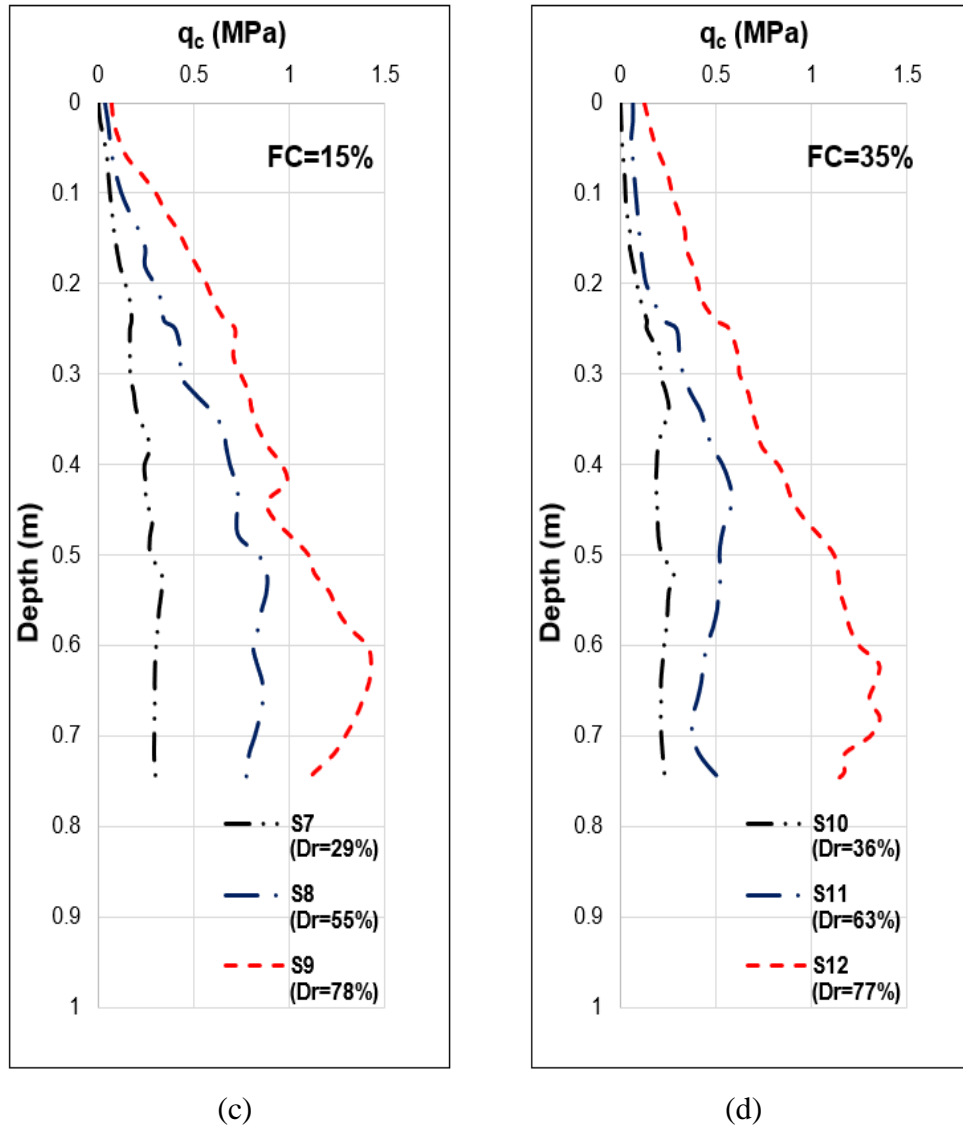
Figure 5.1. Cone penetration resistance data of (a) clean sand (b) %5 silty sand (c) %15 silty sand (d) %35 silty sand with depth.

Determining the soil type index (I_c) is one of the most important applications that can be obtained using CPT data. Soil type index was calculated using the relations and equations given by equations (5.1) to (5.4). I_c values were calculated using equation 5.1 (Robertson and Wride, 1998)

$$I_c = [(3.47 - \log q_{c1})^2 + (\log F_r + 1.22)^2]^{0.5} \qquad (5.1)$$

Where q_{c1} is the normalized cone penetration resistance values when n=1 and F_r is the friction ratio. Normalized cone penetration resistance (q_{c1N}) and F_r are given by equation 5.2 and 5.3 (Robertson and Wride, 1998).

$$q_{c1N} = \left(\frac{q_c}{P_a}\right)\left(\frac{P_a}{\sigma_{vo}'}\right)^n \tag{5.2}$$

$$F_r = \left[\frac{fs}{q_c - \sigma_{vo}}\right]100\% \tag{5.3}$$

Where P_a is the atmospheric pressure, σ_{vo}' is the effective stress, σ_{vo} is the total stress and n is the stress exponent.Stress exponent is calculated by equation 5.4 (Robertson, 2009)

$$n = 0.381(I_c) + 0.05\left(\frac{\sigma_{vo}'}{P_a}\right) - 0.15 \tag{5.4}$$

Table 5.1 shows the data obtained from the CPT experiments. Cone penetration and friction resistance data are obtained from CPT experiments directly. A total of 36 experimental data were obtained from these experiments. Cone penetration resistance values are between 140 kPa and 1714 kPa. Relative density and unit weight of soils were calculated by equations 3.1 and 3.5 in Chapter 3, respectively. Total vertical stress was calculated by equation 5.5. Total vertical and effective stresses are equal since there is no water in the experiments.

$$\text{Total Vertical Stress } (\sigma vo) = \text{Depth} * \text{Unit Weight} \tag{5.5}$$

Table 5.2 shows the q_{c1}, F_r, n and q_{c1N} parameters obtained using equations 5.2, 5.3 and 5.4 and used in soil type index calculation. In this study, soil type index values varied between 1.41 and 2.73.

Table 5.1. Data obtained from the CPT tests

Sample No	FC	SCPT Depth	D_r	Density	σ_{vo}	q_c	f_s
-	%	m	%	kN/m^3	kPa	kPa	kPa
S1		0.25	34		3.40	163	4.00
		0.50	34	13.59	6.80	261	4.00
		0.75	34		10.19	278	5.67
S2	0	0.25	62		3.55	426	2.99
		0.50	62	14.18	7.09	863	2.99
		0.75	62		10.64	874	4.00
S3		0.25	87		3.69	581	2.99
		0.50	87	14.74	7.37	1190	2.99
		0.75	87		11.06	1714	4.00
S4		0.25	35		3.50	148	4.00
		0.50	35	14.01	7.00	210	4.00
		0.75	35		10.51	228	5.70
S5	5	0.25	55		3.60	459	2.99
		0.50	55	14.41	7.20	781	2.99
		0.75	55		10.81	667	4.00
S6		0.25	75		3.71	648	4.00
		0.50	75	14.85	7.42	1280	4.00
		0.75	75		11.14	1593	5.67
S7		0.25	29		3.62	167	4.00
		0.50	29	14.49	7.25	275	4.00
		0.75	29		10.87	306	5.70
S8	15	0.25	55		3.79	405	4.00
		0.50	55	15.15	7.58	838	4.00
		0.75	55		11.36	767	5.70
S9		0.25	78		3.95	717	4.23
		0.50	78	15.79	7.90	1100	4.23
		0.75	78		11.84	1087	5.70
S10		0.25	36		3.87	140	4.00
		0.50	36	15.48	7.74	220	4.00
		0.75	36		11.61	228	5.70
S11	35	0.25	63		4.13	296	2.99
		0.50	63	16.54	8.27	520	2.99
		0.75	63		12.40	543	4.00
S12		0.25	77		4.29	570	4.00
		0.50	77	17.16	8.58	1118	4.00
		0.75	77		12.40	1112	5.67

Table 5.2. The parameters used in the soil type index calculation

Sample No	FC	SCPT Depth	q_{c1}	F_r	I_c	n	q_{c1N}
-	%	m	-	%	-	-	-
S1	0	0.25	47.97	2.51	2.41	0.77	22.11
		0.50	38.41	1.57	2.36	0.75	19.71
		0.75	27.27	2.12	2.55	0.83	18.43
S2		0.25	120.15	0.71	1.75	0.52	24.20
		0.50	121.70	0.35	1.58	0.46	28.84
		0.75	82.17	0.46	1.79	0.54	29.13
S3		0.25	157.65	0.52	1.58	0.45	25.93
		0.50	161.45	0.25	1.41	0.39	32.89
		0.75	155.03	0.23	1.41	0.39	40.68
S4	5	0.25	42.26	2.77	2.48	0.80	21.44
		0.50	29.98	1.97	2.50	0.81	17.96
		0.75	21.70	2.62	2.69	0.88	16.57
S5		0.25	127.43	0.66	1.71	0.50	24.58
		0.50	108.41	0.39	1.65	0.48	27.67
		0.75	61.72	0.61	1.96	0.60	25.41
S6		0.25	174.57	0.62	1.59	0.46	29.32
		0.50	172.41	0.31	1.43	0.40	35.97
		0.75	143.05	0.36	1.53	0.44	41.55
S7	15	0.25	46.09	2.45	2.42	0.77	21.73
		0.50	37.95	1.49	2.35	0.75	19.62
		0.75	28.15	1.93	2.52	0.82	18.70
S8		0.25	106.92	1.00	1.89	0.57	26.24
		0.50	110.62	0.48	1.69	0.50	30.20
		0.75	67.50	0.75	1.97	0.61	28.77
S9		0.25	181.60	0.59	1.57	0.45	30.56
		0.50	139.31	0.39	1.55	0.45	34.09
		0.75	91.77	0.53	1.78	0.53	33.94
S10	35	0.25	36.17	2.94	2.55	0.82	20.38
		0.50	28.42	1.88	2.51	0.81	17.49
		0.75	19.63	2.64	2.73	0.89	15.64
S11		0.25	71.59	1.02	2.03	0.63	21.72
		0.50	62.88	0.58	1.94	0.59	22.84
		0.75	43.78	0.75	2.13	0.67	21.93
S12		0.25	132.88	0.71	1.72	0.51	28.16
		0.50	130.32	0.36	1.56	0.45	33.71
		0.75	86.41	0.52	1.79	0.54	33.66

Figure 5.2 shows the soil type index data of clean sand, 5% silty soil, 15% silty soil and 35% silty soil at different relative density (D_r) data obtained from CPT test parameters.

Figure 5.2 (a). shows the soil type index (I_c) data along with the depth for FC=0%. The figure shows the soil with three different relative densities (D_r) as 34%, 62%, and %87. The D_r of sample 1 is 34%, and the average soil type index value is 2.29. The D_r of sample 2 is 62%, and average soil type index value is 1.72. The D_r of sample 3 is 87%, and average soil type index value is 1.48.

Figure 5.2 (b). shows the soil type index (I_c) data along with the depth for FC=5%. The figure shows the soil with three different relative densities (D_r) as 35%, 55% and %75. The D_r of sample 4 is 35%, and average soil type index value is 2.48. The D_r of sample 5 is 55%, and average soil type index value is 1.72. The D_r of sample 6 is 75%, and average soil type index value is 1.47.

Figure 5.2 (c). shows the soil type index (I_c) data along with the depth for FC=15%. The figure shows the soil with three different relative densities (D_r) as 29%, 55% and %78. The D_r of sample 7 is 29%, and average soil type index value is 2.35. The D_r of sample 8 is 55%, and average soil type index value is 1.80. The D_r of sample 9 is 78%, and average soil type index value is 1.54.

Figure 5.2 (d). shows the soil type index (I_c) data along with the depth for FC=35%. The figure shows the soil with three different relative densities (D_r) as 36%, 63% and %77. The D_r of sample 10 is 36%, and average soil type index value is 2.59. The D_r of sample 11 is 63%, and average soil type index value is 2.05. The D_r of sample 12 is 77%, and average soil type index value is 1.60.

In general, soil type index values (I_c) increased as the relative density decreased for each experiment with different fines content (FC). Also, I_c increases as the fineness content (FC) increases. As can be seen in Figure 5.2, the plots shifted to the right as FC increased.
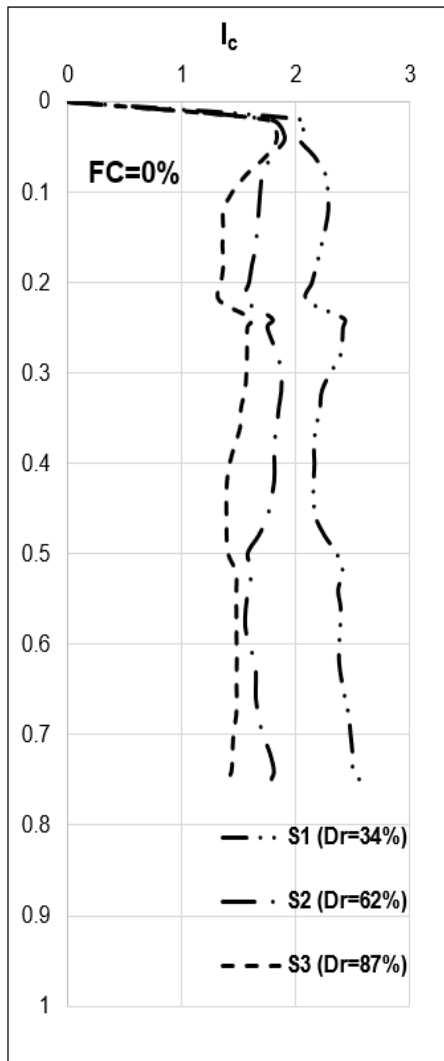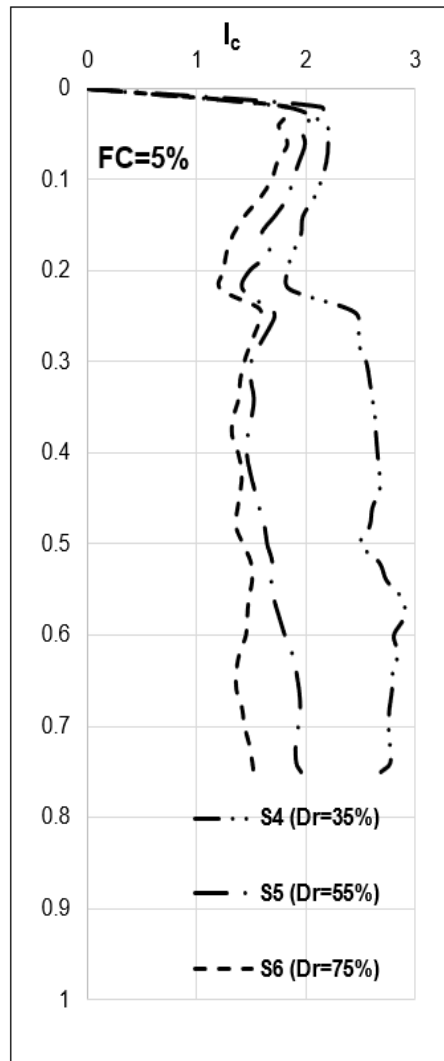
(a)   (b)
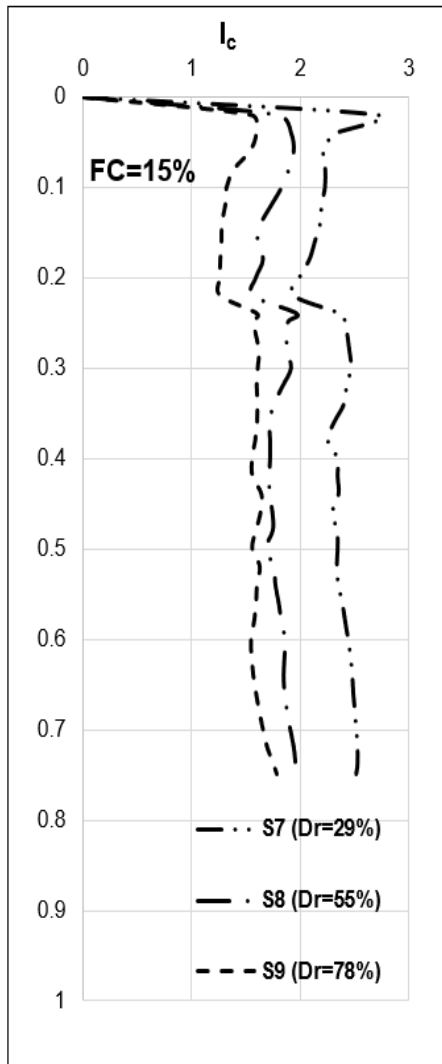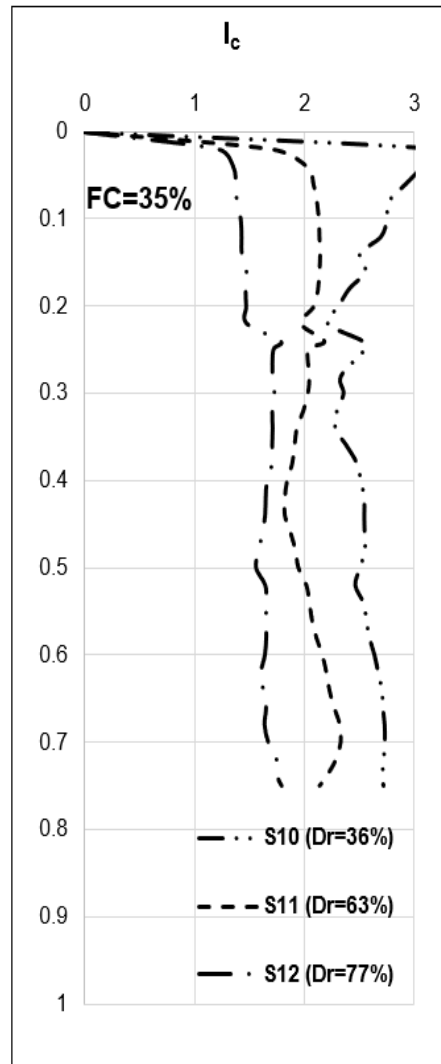
(c)   (d)

Figure 5.2. Soil type index data of (a) clean sand (b) %5 silty sand (c) %15 silty sand (d) %35 silty sand with depth.

5.3. Shear wave velocity

Shear wave measurements were found by seismic CPT (SCPT). Shear wave calculations were made using the cross-correlation method by using the Geotech SPT software. The cross-correlation method was preferred because it works at low signals, gives fast and detailed results, and uses the entire signal of the shear waves. Shear waves were generated when the hammer hit the S-plate at measured depths. The shear wave was calculated by dividing the distance of the waves formed at these depths from the seismic adapter by the time between the two waves. Figure 5.3 shows a schematic view of SCPT experiments and the calculation of shear wave velocity. L1 and L2 show the distance between the generated shear waves and the seismic adapter, while D1 and D2 show the vertical distance of the SCPT tests. X denotes the distance between the S-plate and the CPT rod; in this study, X is 100 cm.
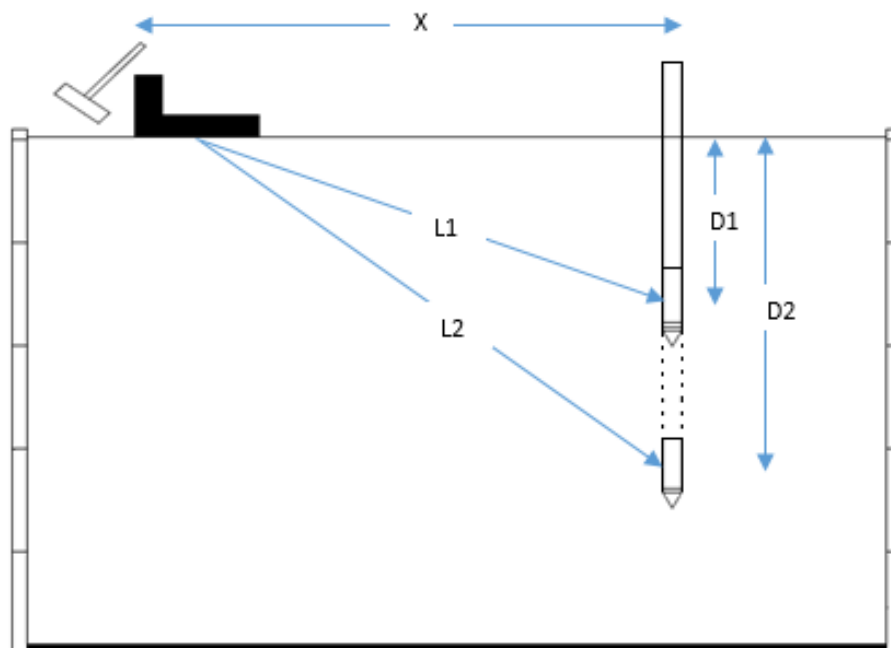
Figure 5.3. Schematic view of SCPT experiments and the calculation of shear wave velocity

In the experiments, SCPT depths were determined at 0.25m, 0.50m, and 0.75 m. The cross-correlation method was used for all shear wave signals between depths of 0.25 meters and 0.50 m and between depths of 0.50 m and 0.75 m. As an example, Figure 5.4

shows the cross-correlation method at a depth of 0.25 m and 0.50 m in 35% silty dense sand. Shear velocity is calculated by equation 5.6.
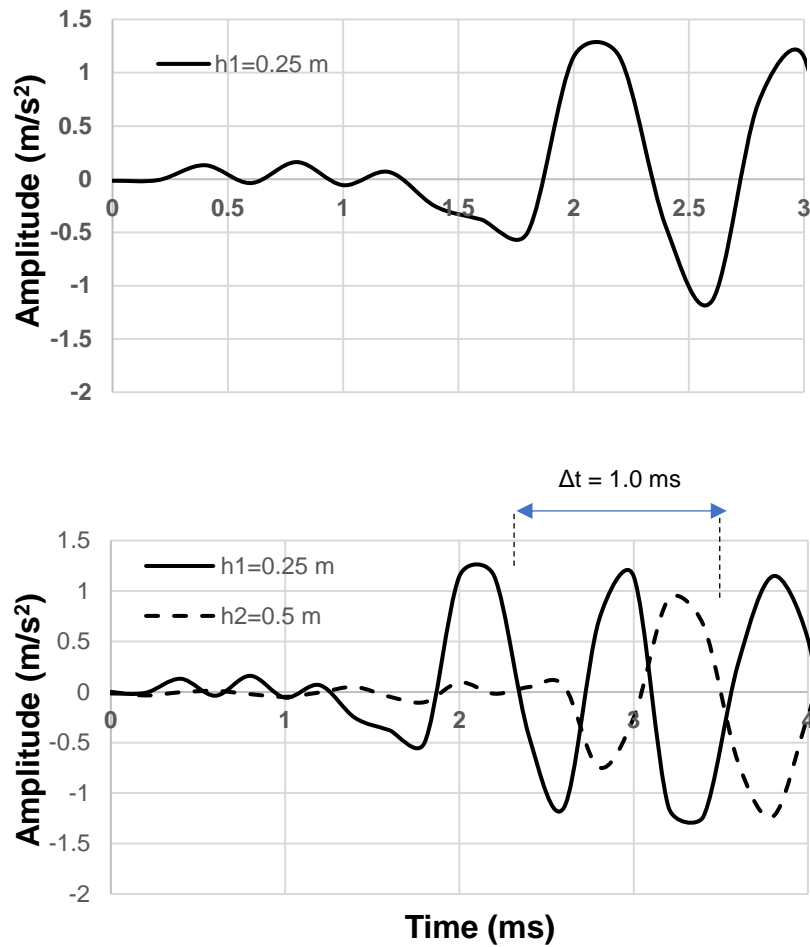
Figure 5.4. Cross-correlation method at a depth of 0.25 meters and 0.50 meters in dense 35% silty sand.

$$\text{Shear Velocity } (V_s) = \frac{\text{Distance of the waves (L2−L1)}}{\text{Time between the waves (∆t)}} \tag{5.6}$$

As seen in Figure 5.4, the time elapsed between the first peak point of the shear wave generated at 0.25 m depth and the first peak point generated at 0.5 m depth is 1.0 ms. The only unknown in equation 5.6 is the distance of the waves. SCPT analysis software gives the distance between two waves. Figure 5.5 shows the analysis result of dense 35% silty sand. The distance of the waves is denoted as D2 – D1(corr) in analysis

software. The distance of the waves is 0.09 m. The shear wave was found as 90 m/s for 35 % silty dense sand using the Equation 5.6.
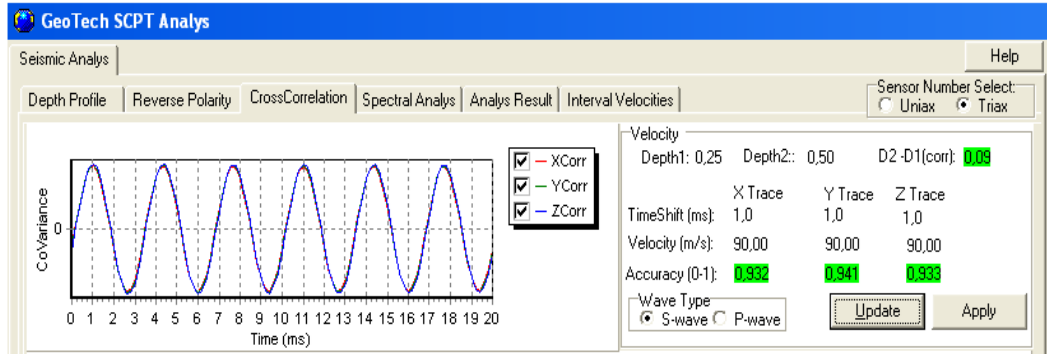
Figure 5.5. SCPT Analysis program (Geotech SCPT) results of dense 35% silty sand.

The filtering process was applied while the SCPT test results were analyzed using the cross-correlation method. The filtering process cleans the external sounds that may occur during the experiment and the vibrations caused by the experimenter's movements. Filtering was done in Geotech SCPT analysis software by using Band Pass Filter (Hz) option. Low and high pass frequency values are entered into the system using the band pass filter option. The low and high pass frequency values entered into the system are limit values. Frequency values between 140 Hz and 320 Hz were entered into the system. As the frequency values change during the filtering process, the accuracy values also change. During the operations, care was taken to ensure that the accuracy value was between 0.9 and 1. Figure 5.6 shows the shear wave velocity data of clean sand, 5% silty soil, 15% silty soil and 35% silty soil at different relative densities. Seismic experiments were applied to 4 different soil samples, 12 shear wave profiles were obtained, and shear wave values were found to be between 75 m/s and 108 m/s.

Figure 5.6 (a) shows the shear wave velocity (V_s) data along the depth for FC=0%. The figure shows the soil with three different relative densities (D_r) as 34 %, 62 % and % 87. The D_r of sample 1 is 34 %, and V_s is 90 m/s between 0.25 m and 0.50 m depths and 108 m/s between 0.50 m and 0.75 m depths. The D_r of sample 2 is 62 %, and V_s is 75 m/s between 0.25 m and 0.50 m depths and 90 m/s between 0.50 m and 0.75 m depths. The D_r of sample 3 is 87 %, and V_s is 75 m/s between 0.25 m and 0.50 m depths and 90 m/s between 0.50 m and 0.75 m depths.

Figure 5.6 (b) shows the shear wave velocity (V_s) data along the depth for FC=5%. The figure shows the soil with three different relative densities (D_r) as 35 %, 55 % and % 75. The D_r of sample 4 is 35 %, and V_s is 90 m/s between 0.25 m and 0.50 m depths and 108 m/s between 0.50 m and 0.75 m depths.The D_r of sample 5 is 55 %, and V_s is 75 m/s between 0.25 m and 0.50 m depths and 90 m/s between 0.50 m and 0.75 m depths. The D_r of sample 6 is 75 % and V_s is 90 m/s between 0.25 m and 0.50 m depths and 108 m/s between 0.50 m and 0.75 m depths.

Figure 5.6 (c). shows the shear wave velocity (V_s) data along the depth for FC=15%. The figure shows the soil with three different relative densities (D_r) as 29 %, 55 %, and % 78. The D_r of sample 7 is 29 % and V_s is 90 m/s between 0.25 m and 0.50 m depths and 108 m/s between 0.50 m and 0.75 m depths.The D_r of sample 8 is 55 %, and V_s is 90 m/s between 0.25 m and 0.50 m depths and 108 m/s between 0.50 m and 0.75 m depths. The D_r of sample 9 is 78 %, and V_s is 93 m/s between 0.25 m and 0.50 m depths and 108 m/s between 0.50 m and 0.75 m depths.

Figure 5.6 (d) shows the shear wave velocity (V_s) data along the depth for FC=35%. The figure shows the soil with three different relative densities (D_r) as 36 %, 63 % and % 77. The D_r of sample 10 is 36 % and V_s is 90 m/s between 0.25 m and 0.50 m depths and 108 m/s between 0.50 m and 0.75 m depths. The D_r of sample 11 is 63 % and V_s is 75 m/s between 0.25 m and 0.50 m depths and 90 m/s between 0.50 m and 0.75 m depths. The D_r of sample 12 is 77 % and V_s is 90 m/s between 0.25 m and 0.50 m depths and 108 m/s between 0.50 m and 0.75 m depths.

The V_s values between 0.25 m and 0.5 m were found to be 75 m/s and 90 m/s and between 0.5 m and 0.75 m were found to be 90 m/s and 108 m/s. In general V_s values increased throughout depth for each experiment with different FC.
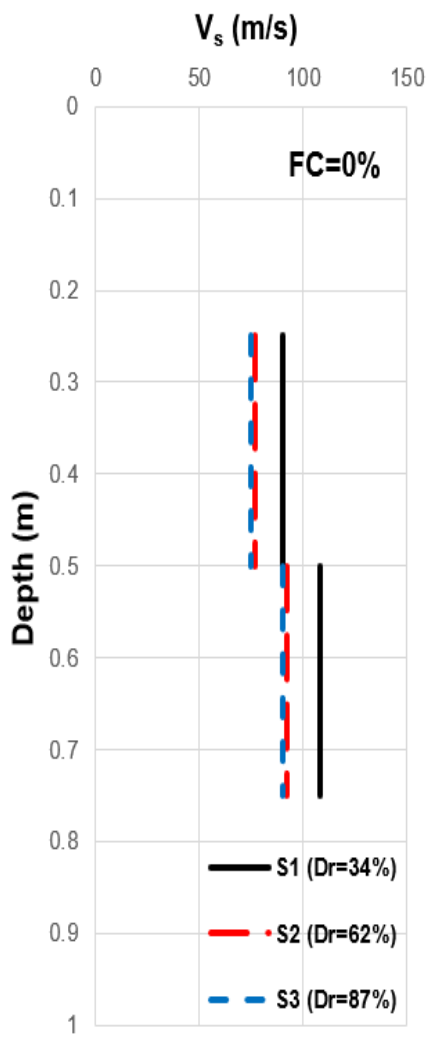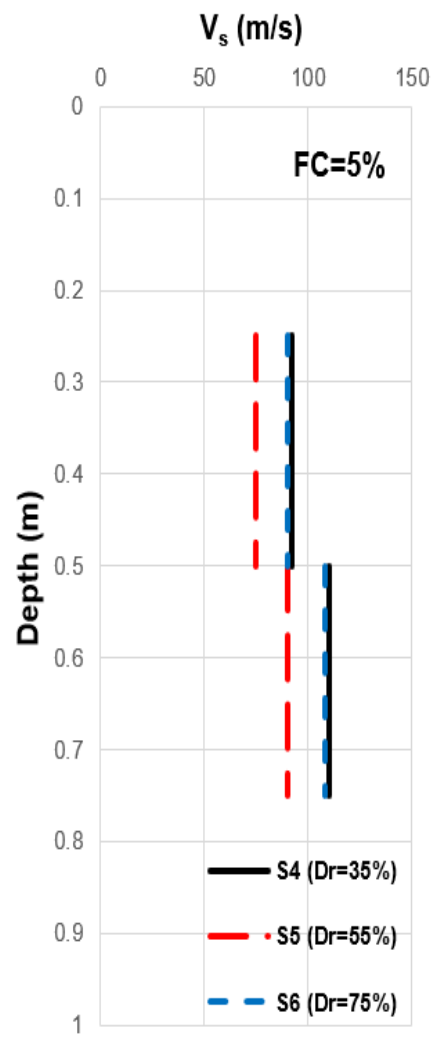
(a)   (b)
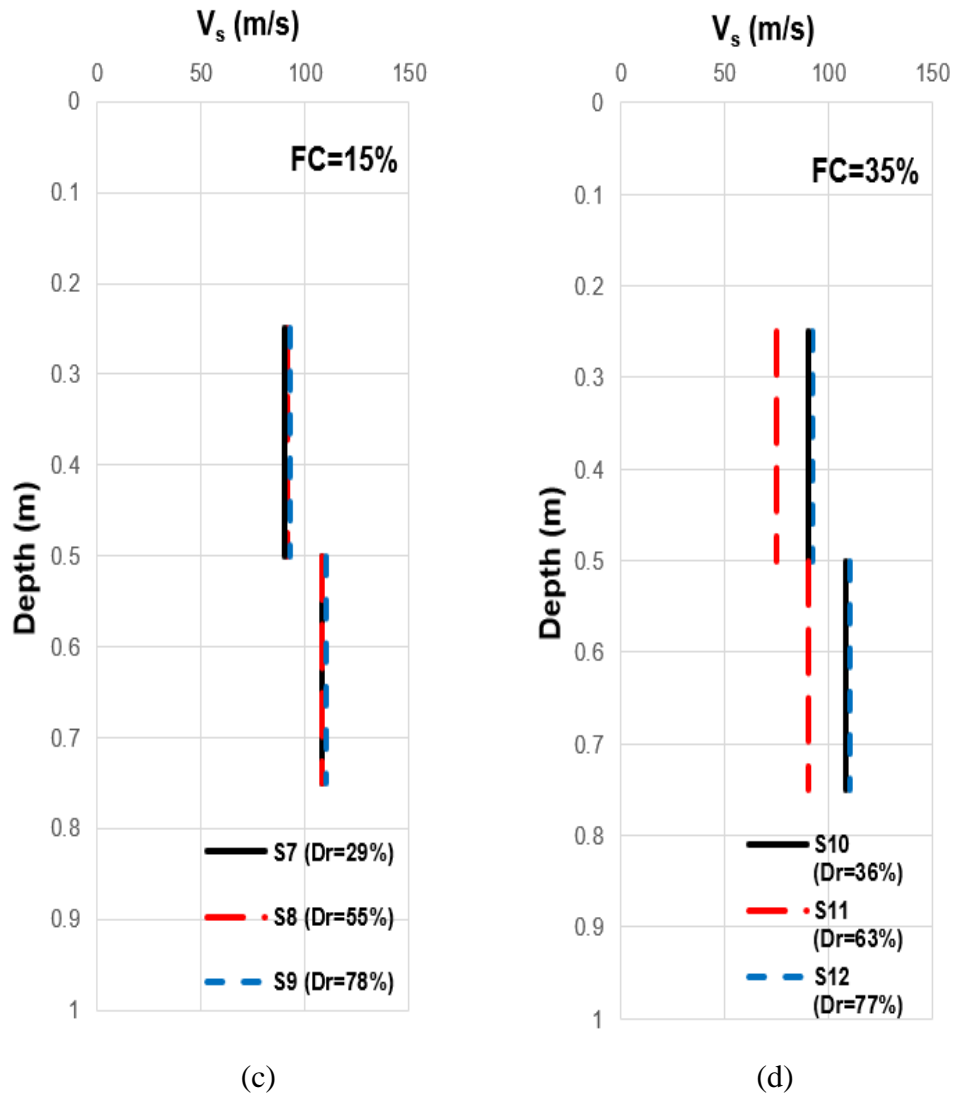
Figure 5.6. Shear wave velocity data of (a) clean sand (b) 5% silty sand (c) 15% silty sand (d) 35% silty sand with depth.

Total of 61 shear wave velocity data were used to determine the relationship between q_c and V_s at different I_c values. 36 of these data are obtained from this study, and 25 data were obtained from the experimental studies of Arık (2021). The experimental data of this study are shown with S, and Arık (2021) data are represented by `MA`. Table 5.3 shows the measured q_c values and V_s values of the data obtained in this study and from Arık (2021) studies.

Table 5.3. Measured cone penetration resistance values and calculated shear wave velocity values of the data obtained in this study and from the studies of Arık (2021).

Sample No	Fines content, FC	Relative Density, D_r	SCPT Depth	Cone penetration resistance, q_c	Shear-wave velocity, V_s
-	%	%	m	kPa	m/sec
S1		34	0.25	163	90
			0.5	261	90
			0.75	278	108
S2		62	0.25	426	75
			0.5	863	75
			0.75	874	90
S3	0	87	0.25	581	75
			0.5	1190	75
			0.75	1714	90
MA1		18	0.4	231	74
			0.8	272	74
			1.2	225	74
S4		35	0.25	148	90
			0.5	210	90
			0.75	228	108
S5		55	0.25	459	75
			0.5	781	75
			0.75	667	90
S6	5	75	0.25	648	90
			0.5	1280	90
			0.75	1593	108
MA4		18	0.4	85	71
			0.8	177	108
MA5		31	0.4	105	83
			0.8	317	100
			1.2	518	100
MA6		77	0.4	2324	110

(cont. on next page)

Table 5.3 (cont.)

Sample No	Fines content, FC	Relative Density, D_r	SCPT Depth	Cone penetration resistance, q_c	Shear-wave velocity, V_s
-	%	%	m	kPa	m/sec
S7		29	0.25	167	90
			0.5	275	90
			0.75	306	108
S8		55	0.25	405	90
			0.5	838	90
			0.75	767	108
S9		78	0.25	717	93
			0.5	1100	93
	15		0.75	1087	108
MA7		21	0.4	73	67
			0.8	95	100
MA8		38	0.4	412	71
			0.8	581	88
			1.2	603	88
MA9		46	0.4	367	77
			0.8	544	100
			1.2	559	100
S10		36	0.25	140	90
			0.5	220	90
			0.75	228	108
S11		63	0.25	296	75
			0.5	520	75
			0.75	543	90
S12		77	0.25	570	90
			0.5	1118	90
	35		0.75	1112	108
MA10		23	0.4	506	83
			0.8	266	88
			1.2	439	88
MA11		32	0.4	247	67
			0.8	440	93
			1.2	468	93
MA12		79	0.3	265	86
			0.6	806	86

Hardin et al. (1972) stated that shear wave velocity is correlated with effective stress. Therefore, shear wave velocity was normalized with the equation given below (Robertson et al., 1992);

$$V_{s1} = V_s \left(\frac{P_a}{\sigma_{vo}'}\right)^{0.25} \tag{5.7}$$

In equation 5.7, P_a represents the atmospheric pressure in the same units as σ_{vo}'. V_s is measured shear wave velocity and σ_{vo}' is effective total stress. Table 5.4 shows the normalized shear wave velocity values (V_{s1}) and normalized cone penetration resistance (q_{c1N}) values of the data obtained in this study and the data obtained from Arık (2021).

Table 5.4. V_{s1} and q_{c1N} values of the data obtained in this study and the data obtained from Arık (2021) studies.

Sample No	Fines content, FC	Relative Density, D_r	SCPT Depth	q_{c1N}	V_s	σ_{vo}'	V_{s1}
-	%	%	m	kPa	m/sec	kPa	m/sec
S1		34	0.25	22.11	90	3.40	209.63
			0.5	19.71	90	6.80	176.27
			0.75	18.43	108	10.19	191.14
S2		62	0.25	24.20	75	3.55	172.84
			0.5	28.84	75	7.09	145.34
	0		0.75	29.13	90	10.64	157.59
S3		87	0.25	25.93	75	3.69	171.18
			0.5	32.89	75	7.37	143.94
			0.75	40.68	90	11.06	156.08
MA1		18	0.4	21.73	74	3.12	176.24
			0.8	19.31	74	6.08	149.16
			1.2	15.34	74	9.28	134.20
S4		35	0.25	21.44	90	3.50	208.05
			0.5	17.96	90	7.00	174.95
			0.75	16.57	108	10.51	190.28
S5		55	0.25	24.58	75	3.60	172.16
			0.5	27.67	75	7.20	144.77
			0.75	25.41	90	10.81	156.97
S6		75	0.25	29.32	90	3.71	205.04
	5		0.5	35.97	90	7.42	172.42
			0.75	41.55	108	11.14	186.96
MA4		18	0.4	19.39	71	2.59	176.98
			0.8	22.23	108	5.03	228.05
MA5		31	0.4	19.57	83	3.38	193.57
			0.8	23.66	100	5.88	203.07
			1.2	25.21	100	8.68	184.23
MA6		77	0.4	45.55	110	6.64	179.27

(cont. on next page)

Table 5.4 (cont.)

Sample No	Fines content, FC	Relative Density, D_r	SCPT Depth	q_{c1N}	V_s	σ_{vo}'	V_{s1}
-	%	%	m	kPa	m/sec	kPa	m/sec
S7		29	0.25	21.73	90	3.62	206.28
			0.5	19.62	90	7.25	173.46
			0.75	18.70	108	10.87	188.66
S8		55	0.25	26.24	90	3.79	204.01
			0.5	30.20	90	7.58	171.55
			0.75	28.77	108	11.36	186.58
S9		78	0.25	30.56	93	3.95	208.32
			0.5	34.09	93	7.90	175.18
	15		0.75	33.94	108	11.84	184.66
MA7		21	0.4	19.73	67	2.2	173.11
			0.8	20.28	100	4.1	222.23
MA8		38	0.4	23.81	71	2.84	174
			0.8	27.82	88	4.64	188.53
			1.2	26.35	88	7.44	167.54
MA9		46	0.4	23.11	77	4.35	168.43
			0.8	29.59	100	4.55	216.52
			1.2	27.80	100	6.75	196.19
S10			0.25	20.38	90	3.87	202.90
		36	0.5	17.49	90	7.74	170.62
			0.75	15.64	108	11.61	185.57
S11			0.25	21.72	75	4.13	166.32
		63	0.5	22.84	75	8.27	139.86
			0.75	21.93	90	12.40	151.65
S12			0.25	28.16	90	4.29	197.76
		77	0.5	33.71	90	8.58	166.30
	35		0.75	33.66	108	12.40	180.32
MA10			0.4	24.38	83	6.82	162.42

5.4. Influence of soil type on q_c – V_{s1} correlation

Popular soil classification systems are based on physical properties such as grain size and plasticity. Since existing classification systems are based on physical properties, they can not fully establish a strong relationship with in-situ behavior (Robertson, 2016). Soil type index data obtained from CPT experiments is a better parameter than existing soil classification systems in determining soil behavior (Robertson, 2009).

In this study, soil type index values were calculated using equation 5.1. A total of 61 experimental data are available and 25 of them were taken from Arık's (2021) studies. Minimum I_c value is 1.30, and the maximum I_c value is 2.95 with the added 25 data. Table 5.5 shows the q_{c1N} values, V_{s1} values and I_c values of the data obtained in this study and the data taken from Arık's (2021) studies.

Table 5.5. q_{c1N} values, V_{s1}, and I_c values of the data obtained in this study and the data taken from Arık's (2021) studies.

Sample No	Fines content, FC	Relative Density, D_r	SCPT Depth	q_{c1N}	V_{s1}	I_c
-	%	%	m	kPa	m/sec	-
S1		34	0.25	22.11	209.63	2.41
			0.5	19.71	176.27	2.36
			0.75	18.43	191.14	2.55
S2		62	0.25	24.20	172.84	1.75
			0.5	28.84	145.34	1.58
			0.75	29.13	157.59	1.79
S3	0	87	0.25	25.93	171.18	1.58
			0.5	32.89	143.94	1.41
			0.75	40.68	156.08	1.41
MA1		18	0.4	21.73	176.24	2.09
			0.8	19.31	149.16	2.22
			1.2	15.34	134.20	2.5
S4		35	0.25	21.44	208.05	2.48
			0.5	17.96	174.95	2.5
			0.75	16.57	190.28	2.69
S5		55	0.25	24.58	172.16	1.71
			0.5	27.67	144.77	1.65
			0.75	25.41	156.97	1.96
S6		75	0.25	29.32	205.04	1.59
	5		0.5	35.97	172.42	1.43
			0.75	41.55	186.96	1.53
MA4		18	0.4	19.39	176.98	2.64
			0.8	22.23	228.05	2.61
MA5		31	0.4	19.57	193.57	2.66
			0.8	23.66	203.07	2.25
			1.2	25.21	184.23	2.08
MA6		77	0.4	45.55	179.27	1.3

Table 5.5 (cont.)

Sample No	Fines content, FC	Relative Density, D_r	SCPT Depth	q_{c1N}	V_{s1}	I_c
-	%	%	m	kPa	m/sec	-
S7		29	0.25	21.73	206.28	2.42
			0.5	19.62	173.46	2.35
			0.75	18.70	188.66	2.52
S8		55	0.25	26.24	204.01	1.89
			0.5	30.20	171.55	1.69
			0.75	28.77	186.58	1.97
S9		78	0.25	30.56	208.32	1.57
			0.5	34.09	175.18	1.55
	15		0.75	33.94	184.66	1.78
MA7		21	0.4	19.73	173.11	2.66
			0.8	20.28	222.23	2.9
MA8		38	0.4	23.81	174	1.68
			0.8	27.82	188.53	1.73
			1.2	26.35	167.54	1.87
MA9		46	0.4	23.11	168.43	1.93
			0.8	29.59	216.52	1.83
			1.2	27.80	196.19	1.95
S10		36	0.25	20.38	202.90	2.55
			0.5	17.49	170.62	2.51
			0.75	15.64	185.57	2.73
S11		63	0.25	21.72	166.32	2.03
			0.5	22.84	139.86	1.94
			0.75	21.93	151.65	2.13
S12		77	0.25	28.16	197.76	1.72
			0.5	33.71	166.30	1.56
	35		0.75	33.66	180.32	1.79
MA10		23	0.4	24.38	162.42	1.92
			0.8	23.45	196.53	2.17
			1.2	24.38	175.86	2.01
MA11		32	0.4	19.26	144.13	2.15
			0.8	20.24	158.44	2.26
			1.2	17.27	142.35	2.38
MA12		79	0.3	22.80	191.71	2.15
			0.6	29.02	161.71	1.71

Figure 5.7 shows the V_{s1} and corresponding q_{c1N} values of the experimental data. The data were divided into three regions according to soil type index values. The first region has data with an I_c value between 1.3 and 1.57. Two black curves bound the area with I_c values of 1.3 and 1.57, and there are 7 data in this region. The data in this region are shown with blue circles. The second region has data with an I_c value between 1.57

and 1.95. Two black curves bound the area with I_c values of 1.57 and 1.95, with 21 data in this region. Data in this region are shown with orange squares. The third region has data with an Ic value between 1.95 and 2.90. Two black curves bound the area with I_c values of 1.95 and 2.90, with 33 data in this region. Data in this region are shown with black triangles.
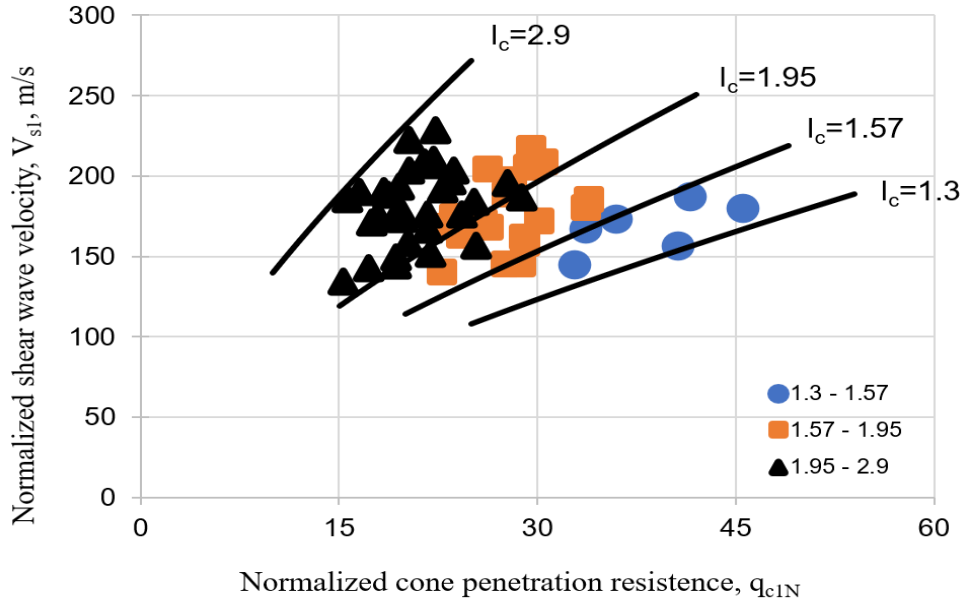

Figure 5.7. Relationship between V_{s1} with q_{c1N} in four soil type index values

Therefore, four I_c curves with values of 1.30, 1.57, 1.95 and 2.90 were created to predict normalized shear wave velocity. The relationship between V_{s1} and q_{c1N} is proposed as follows:

$$V_{s1} = \sqrt{60 * q_{c1N}^{1.45} * I_c^{2.3}} \qquad (5.8)$$

All experimental data were classified according to Table 5.6 with the formation of I_c curves with values of 1.30, 1.57, 1.95, and 2.90. Table 5.6 shows the soil behavior type limits proposed by Robertson and Wride (1998). Based on the soil type index, all experiment samples are composed of soil with the behavior of clean sand to silty sand ($1.30 < I_c < 2.90$). There is not any soil showing clay behavior ($2.95 < I_c < 3.60$).

Table 5.6. The soil behavior type limits proposed by Robertson and Wride (1998).

Soil type index, I_c	Soil Behaviour type
$I_c < 1.31$	Gravelly sand to dense sand
$1.31 < I_c < 2.05$	Sands: clean sand to silty sand
$2.05 < I_c < 2.60$	Sand mixtures: silty sand to sandy silt
$2.60 < I_c < 2.95$	Silt mixtures: clayey silt to silty clay
$2.95 < I_c < 3.60$	Clays: silty clay to clay

Figure 5.8 (a) and Figure 5.8 (b) compare the proposed q_{c1N}–V_{s1} curves with the existing relationships based on different soils. Figure 5.8 (a) shows the comparison of the curves created by the relationship proposed in this study with the curves created by the relationships offered by Ecemis, (2020), Robertson, (2009), Andrus et al., (2007), and Hegazy and Mayne, (2006) based on the soil type index (I_c). As seen in the figure, for I_c = 1.30, I_c = 1.57, and I_c = 1.95, the curve created with the relationship proposed in this study is above the curves created with the existing relationships. The curve Ecemis (2020) presented for I_c = 2.9 almost coincides with the curve created in this study. For I_c = 2.9, the curve created with the relationship proposed in this study is between the curves presented with the existing relationship and showed an average trend.

Figure 5.8 (b) shows the comparison of the curves created by the relationship proposed in this study with the curves created by the relationships offered by Baldi et al. (1989), Rix and Stokoe (1991), Robertson et al. (1992), Fear and Robertson (1995), Hegazy and Mayne (1995), Andrus et al. (2004), Karray et al. (2011), Cai et al. (2014) based on the different soils.

The figure 5.8 (b) also shows the soil type index values of the soils used by the researchers while developing the relationships. Baldi et al. (1989) developed the relationship for uncemented silica sand. According to the Robertson (1990) chart, the uncemented silica sand is classified in terms of behaviour as a sand ($I_c < 2.05$).

Rix and Stokoe (1991) developed a relationship for poorly graded sand and uncemented sand deposits containing between 10% and 20% fines. According to the Robertson (1990) chart, the poorly graded sand is classified in terms of behaviour as a sand ranging from gravelly sand to dense sand ($I_c < 1.31$) and the uncemented sand deposits are classified in terms of behaviour as a silty sand to sandy silt ($2.05 < I_c < 2.60$).

Robertson et al. (1992) developed a relationship for young, uncemented silica clean sand. According to the Robertson (1990) chart, the young, uncemented silica clean sand is classified in terms of behaviour as a sand ranging from clean sand to silty sand $(1.31 < I_c < 2.05)$.

Fear and Robertson (1995) developed a relationship for sand consisting of carbonate shell material and containing 30% fines. According to the Robertson (1990) chart, the sand consisting of carbonate shell material and containing 30% fines is classified in terms of behaviour as a sand mixtures $(I_c > 2.05)$.

Hegazy and Mayne (1995) developed a relationship for sand deposites. According to the Robertson (1990) chart, the sand deposits are classified in terms of behaviour as a sand ranging from clean sand to silty sand $(1.31 < I_c < 2.05)$.

Andrus et al. (2004) developed a relationship for uncemented holocene sand. According to the Robertson (1990) chart, the sand is classified in terms of behaviour as a sand ranging from clean sand to silty sand $(1.31 < I_c < 2.25)$.

Karray et al. (2011) developed a relationship for uncemented and holocene age granular soils. According to the Robertson (1990) chart, the soils are classified in terms of behaviour as a sand ranging from clean sand to silty sand $(1.31 < I_c < 2.05)$.

Cai et al. (2014) developed a relationship for Clay deposits. According to the Robertson (1990) chart, the clay deposits are classified in terms of behaviour as clay ranging from silty clay to clay $(2.95 < I_c < 3.60)$.

The existing relationships proposed by researchers are between q_{c1N} and V_{s1}, and the relationships are not I_c-dependent. In this study, the relationship proposed between q_{c1N} and V_{s1} is I_c-dependent. The curves created with the relationship presented in this study showed a more separate and steeper trend than the curves created with the existing relationships. The curves proposed by Rix and Stokoe (1991) and Karray et al. (2011) are above the curves presented by other researchers. It is clear that the curve by Cai et al. (2014) is below the other curves. Cai et al. (2014) developed the relationship for clay deposits. Other seven relationships have been proposed for Holocene age sand. It is clear that the reason for different trends is due to the soil type difference.

The curves in figure 5.8 (b) created with the relationship developed in this study showed a more separate and steeper trend than the other curves. The reason for this difference is that the other relationships compared are not dependent on the soil type index. The curves in figure 5.8 (a) are closer to each other and show an average trend. Because the curves in this figure are created by soil-type dependent relationships.
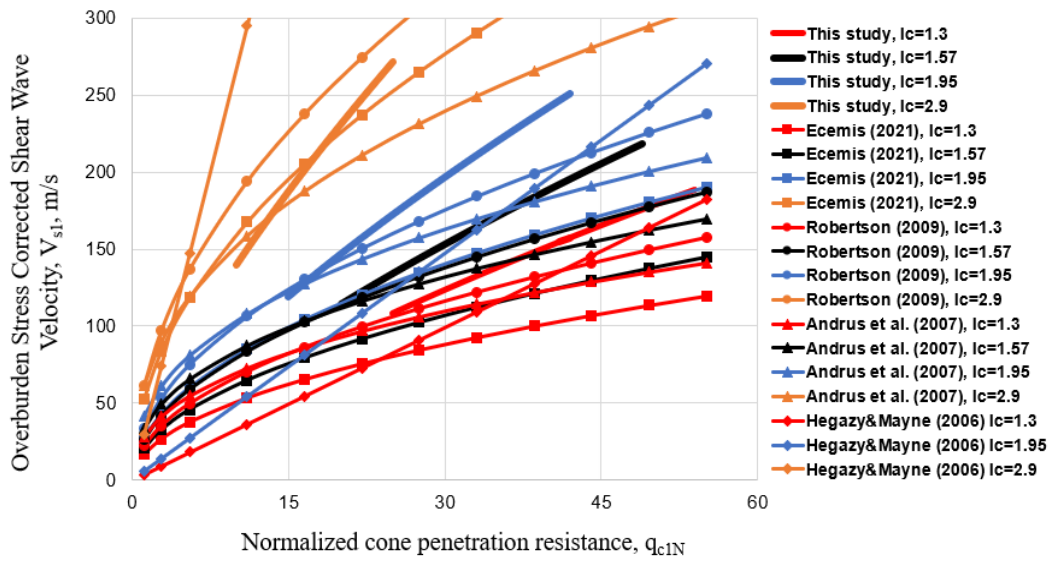
(a)
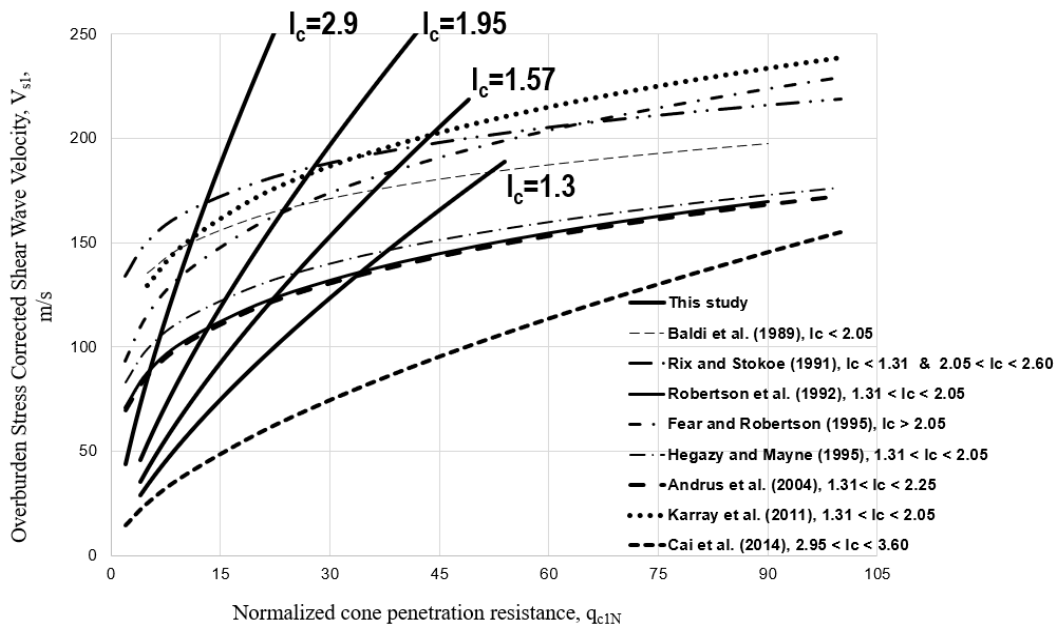
(b)

Figure 5.8. Comparison of the proposed q_{c1N}–V_{s1} curves with the existing relationships based on (a) soil type index (I_c) and (b) different soils

CHAPTER 6

CONCLUSION AND SUGGESTIONS

6.1. Introduction

In this study, the influence of soil type on the correlation between shear wave velocity and cone penetration resistance was investigated by laboratory studies.A total of 12 tests (CPT, SCPT) were applied for clean sand (0% silt), 5% silty sand, 15% silty sand and 35% silty sand for loose, medium dense, and dense states in the soil box. Relative density values were between 29%, and 36% for loose state,%55, and %63 for medium dense,and 75% and 87% for dense state.

The following conclusions were drawn from this study :

- Cone penetration resistance increased throuhout depth. The qc values at D_r=75-87% were 4-5 times greater than at D_r=29-36% and the qc values at D_r=55-63% were 2-3 times greater than at D_r=29-36%. In general, qc increased as the D_r increased for each experiment with different fines content. Also, q_c decreases as the fines content increases.

- There was no significant increase or decrease in V_s values with the change of D_r. SCPT experiments were applied on shear wave measurements and these experiments were carried out in a laboratory. SCPT is an in-situ test and an experiment without a laboratory application, so the small differences in shear wave values might be due to this reason. Also, no significant difference was observed in the V_s values as the fines content changed, so the effect of the fine was not strong on the V_s values.

- Average I_c values at D_r=29-36 are 2.29 to 2.59, avarage I_c values in D_r=55-63 were between 1.72 and 2.05 and average I_c values in Dr=75-87 were between 1.48 and 1.60. In general, I_c values increased as the D_r decreased for each experiment with different fines content. Also, I_c increases as the fines content increased.

- A total of 61 laboratory data pairs were used to develope a variation of V_{s1} with respect to q_{c1N} for different soil type index values of clean sand (0% silt), 5% silty sands, 15% silty sands and 35% silty sands in the laboratory. Four I_c curves with values of 1.30, 1.57, 1.95 and 2.90 were created to predict a corrrelation between V_s and q_{c1N}. Soil type-dependent correlation between q_{c1N} and V_{s1} for silty sand, included quaternary sediments, was proposed as follows :

$$V_{s1} = \sqrt{60 * q_{c1N}^{1.45} * I_c^{2.3}} \qquad (6.1)$$

Where V_{s1} is in m/s. The new equation is useful to estimate V_s from CPT measurements for all soil types.

- As a result of comparing the curves created by the relationship proposed in this study with the curves created by the relationships proposed by other researchers based on different soils; it was observed that the curves created with the relationship presented in this study showed a more separate and steeper trend than the curves created with the existing relationships. The relationship proposed in this study is I_c dependent and the relationship was developed using soils with different FC values. Other curves compared were created with relationships not dependent on I_c. The researchers used only one soil type when developing the relationships and did not use soils with different FC. This difference might explain the position of the curves.

6.2. Suggestions

SCPT test is an in-situ test and laboratory applications are not common. Bender element test or resonant column test can be used for shear wave velocity measurements. The proposed correlation was determined from clean sand and silty sand containing quaternary sediments. Therefore, when calculating shear wave velocity from cone penetration resistance, soil type, depositional environments, geological age, bonding and cementation must be taken into account.

REFERENCES

Andrus, R. D., Piratheepan, P., Ellis, B., Zhang, J. and Juang, C. H. 2004. "*Comparing liquefaction evaluation methods using penetration-V_S relationships*", Soil Dynamics and Earthquake Engineering 24(9-10), 713–721. https://doi.org/10.1016/j.soildyn.2004.06.001.

Andrus, R., Mohanan, N., Piratheepan, P., Ellis, B. and Holzer , T. 2007. "*Predicting shear-wave from cone penetration resistance*", Fourth International Conference on Earthquake Geotechnical Engineering, Thessaloniki, Greece. Paper no.1454

Arık, M. S. 2021. "*Effect of fines content on CPT resistance in silty sands*", [Master thesis, İzmir Institute of Technology]. https://hdl.handle.net/11147/11108

ASTM D5778-12, "Standard test method for electronic friction cone and piezocone penetration testing of soils. ", ASTM, Pennsylvania, 2012, www.astm.org doi:10.1520/D5778-12

Baldi, G., Bellotti, R., Ghionna, V., Jamiolkowski, V. and LoPresti, D. 1989. "*Modulus of sands from CPT sand DMTs*", Proceedings of the 12th International Conference on Soil Mechanics and Foundation Engineering, Rio de Janeiro.Vol. 1, 165-170

Cai, G., Puppala, A. J. and Liu, S. 2014. "*Characterization on the correlation between shear wave velocity and piezocone tip resistance of Jiangsu clays*", Engineering Geology 171, 96–103. https://doi.org/10.1016/j.enggeo.2013.12.012

Ecemis, N. 2020. "*Effect of Soil-Type and Fines Content on Liquefaction Resistance—Shear-wave velocity correlation*", Journal of Earthquake Engineering 24(8), 1311-1335. https://doi.org/10.1080/13632469.2018.1475312

Ecemis, N., Monkul, M. M., Tütüncü, Y. E. and Arık, M. S. 2022. "*CPT-Based Liquefaction Resistance of Clean and Silty Sands: A Drainage conditions Based Approach*", https://doi.org/10.21203/rs.3.rs-1427044/v1

Fear, C.E and Robertson, P.K 1995. "*Estimating the undrained strength of sand: a theoretical framework*", Canadian Geotechnical Journal 32(5), 859-870. https://doi.org/10.1139/t95-082

Hardin, B. O. and Drnevich, V. P. 1972. "*Shear modulus and damping in soils:Measurement and parameter effects (Terzaghi Leture)* ", Journal of the Soil Mechanics and Foundations Division 98(6), 603-624. https://doi.org/10.1061/JSFEAQ.0001756

Hegazy, Y. and Mayne, P. 1995. "*Statistical correlations between Vs and CPT data for different soil types*", Proc. Cone Penetration Testing (CPT'95).Vol. 2, 173-178

Hegazy, Y. A. and Mayne, P. W. 2006. "*Global Statistical Correlation between Shear Wave Velocity and Cone Penetration Data*", Geotechnical Special Publication, 243-248. https://doi.org/10.1061/40861(193)31

Karray, M., Lefebvre, G., Ethier, Y. and Bigras, A. 2011. "*Influence of particle size on the correlation between shear wave velocity and cone tip resistance*", Canadian Geotechnical Journal 48(4), 599-615. https://doi.org/10.1139/t10-092

Lunne, T., Robertson, P. and Powell, J. 1997. "*Cone Penetration Testing in Geotechnical Practice*", Soil Mechanics and Foundation Engineering.

Mayne, P. and Rix, G. 1995. "*Correlations between shear wave velocity and cone tip resistance in natural clays*", Soils and Foundations 35(2), 107-110. https://doi.org/10.3208/sandf1972.35.2_107

Rix, G., & Stokoe, K. 1991. "*Correlation of initial tangent modulus and cone penetration resistance*", Calibration Chamber Testing, 351-362

Robertson, P. 2009. "*Interpretation of cone penetration tests — a unified approach*", Canadian Geotechnical Journal 46(11), 1337-1355. https://doi.org/10.1139/T09-065

Robertson, P. 2010. "*Soil behaviour type from the CPT: an update*", 2nd International Symposium on Cone Penetration Testing, Huntington Beach, CA, USA.

Robertson, P. 2016. "*CPT - based soil behavior type (SBT) classification system - an update*", Canadian Geotechnical Journal 53(12), p.1910. https://doi.org/10.1139/cgj-2016-0044

Robertson, P., & Wride, C. 1998. "*Evaluating cyclic liquefaction potential using the cone penetration test*", Canadian Geotechnical Journal 35(3), 442-459. https://doi.org/10.1139/t98-017

Robertson, P., Campanella, R., Gillespie, D., & Rice, A. 1986. "*Seismic CPT to measure ın-situ shear wave velocity*", Journal of Geotechnical Engineering 112(8). https://doi.org/10.1061/(ASCE)0733-9410(1986)112:8(791)

Robertson, P., Woeller, D., & Finn, W. 1992. "*Seismic cone penetration test for eveluating liquefaction potential under cyclic loading*". Canadian Geotechnical Journal 29, 686-695. https://doi.org/10.1139/t92-075

Schmertmann, J. 1978. "*Guidelines for Cone Penetration Test (Performance and Design)* ", U.S Department of Transportation Federal Highway Administration [Report No : FHWA-TS-78-209], Washington. https://rosap.ntl.bts.gov/view/dot/958

Tonni, L. and Simonini, P. 2013. "*Shear wave velocity as function of cone penetration test measurements in sand and silt mixtures*", Engineering Geology 163, 55-67. https://doi.org/10.1016/j.enggeo.2013.06.005
[Report No : FHWA-TS-78-209], Washington.

Wair, R., DeJong, J. and Shantz, T. 2012. "*Guidelines for estimation of shear wave velocity profiles*", Pacific Earthquake Engineering Research Center Headquarters at the University of California p. 42